Leading edge topography of blades - a critical review

Robert J. K. Wood *, Ping Lu

National Centre for Advanced Tribology, University of Southampton, SO17 1BJ, Southampton, UK

Correspondence: r.wood@soton.ac.uk;

Keywords: Leading edge topography, roughness, additive mechanisms, subtractive mechanisms, turbomachinery, performance degradation

Abstract

In turbomachinery, their blade leading edges are critical to performance and therefore fuel efficiency, emission, noise, running and maintenance costs. Leading edge damage and therefore roughness is either caused by subtractive processes such as foreign object damage (bird strikes and debris ingestion) and erosion (hail, rain droplets, sand particles, dust, volcanic ash and cavitation) and additive processes such as filming (from dirt, icing, fouling, insect build-up). Therefore, this review focuses on the changes in topography induced by during service to blade leading edges and the effect of roughness and form on performance and efforts to predict and model these changes. The applications considered are focused on wind, gas and tidal turbines and turbofan engines. Repair and protection strategies for leading edges of blades are also reviewed. The review shows additive processes are typically worse than subtractive processes, as the roughness or even form change is significant with icing and biofouling. Antagonism is reported between additive and subtractive roughness processes. There are gaps in the current understanding of the additive and subtractive processes that influence roughness and their interaction. Recent work paves the way forward where modelling and machine learning is used to predict coated wind turbine blade leading edge delamination and the effects this has on aerodynamic performance and what changes in blade angle would best capture the available wind energy with such damaged blades. To do this generically there is a need for better understanding of the environment that the blades see and the variation along their length, the material or coated material response to additive and/or subtractive mechanisms and thus the roughness/form evolution over time. This is turn would allow better understanding of the effects these changes have on aerodynamic/ hydrodynamic efficiency and the population of stress raisers and distribution of residual stresses that result. These in turn influence fatigue strength and remaining useful life of the blade leading edge as well as inform maintenance/repair needs.

1. Introduction

In open and enclose turbomachinery (both axial and radial machines), the shape and roughness of the leading edge of the blades is critical to their performance, which includes fuel efficiency, emissions, noise, and operating and maintenance costs. Machines most effected are in the power generation, sustainable energy, aerospace sectors and marine propulsion. Leading edge damage and therefore roughness is typically caused by subtractive processes such as foreign object damage (bird strikes and debris ingestion) and erosion (hail, rain droplets, sand particles, dust, volcanic ash and cavitation) and additive processes such as filming (from dirt, icing, fouling, insect build-up) and is a recognised issue for wind turbines, turbomachinery and rotorcraft. Examples of wind turbine leading edge erosion over a range of years in service are shown in Figure 1. If the subtractive processes are severe, the form (geometry) of the leading edge can also be lost (flattened) and stresses in the blade increased thereby shortening the life of the blade.

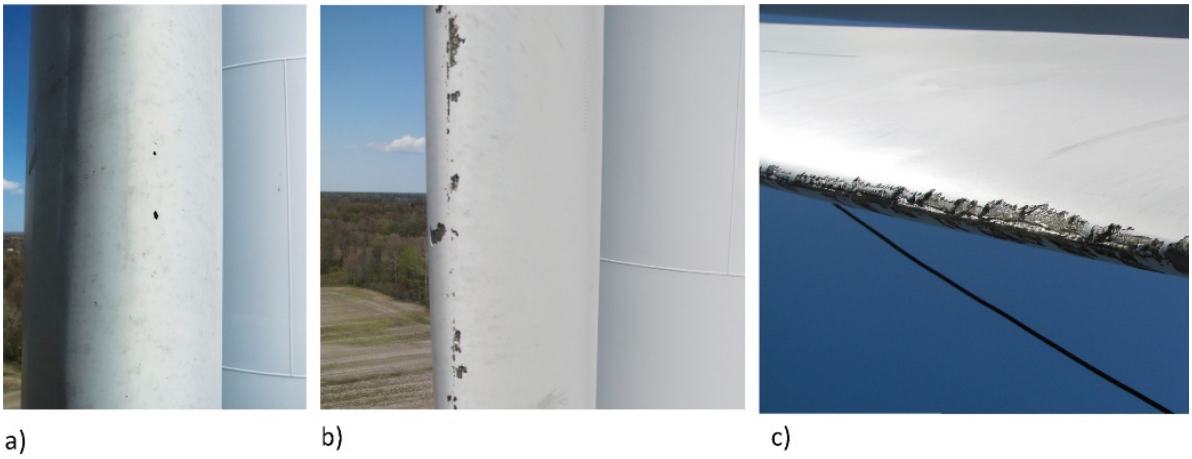

Figure 1 Examples of wind turbine leading edge erosion across a range of years in service [1, 2]

The fuel burn data from an aeroengine test with eroded and redressed fan blades has recently been made available. Based on the combined effect of the different degrees in efficiency loss across the engine cycle, a 1% increase in fuel burn was seen due to erosion of the leading edges [3]. If this erosion can be eliminated and by using typical flight data from USA mainland and regional commercial carriers then fuel savings between 80M and 100M gal per year and drops in emissions by 750 M to 1B kg CO_2 pa and 700 M to 1B kg NOx pa are predicted [4], see Figure 2.

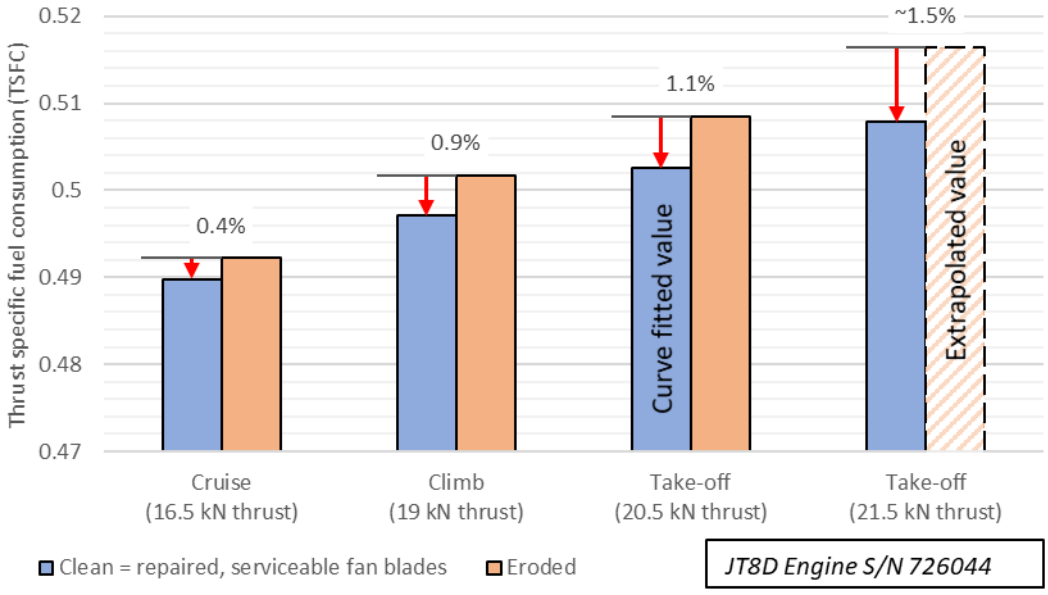

Figure 2 Thrust specific fuel consumption (TSFC) comparison of eroded vs. serviceable fan blades, adopted from [3]

For rotorcraft, significant rain erosion of the leading edges occurs even at subsonic speeds [5]. Loss of initial surface roughness and subsequent loss of profile directly effects the aerodynamic efficiency and thus power generation, lift and thrust. Roughening or changing the form (profile) of the leading edge will increase the overall lifetime cost by increasing performance losses, emissions (increased fuel consumption due to reduced aerodynamic efficiency), and reduced system life and increased maintenance requirements. A related knock-on effect is increased noise and vibration caused by leading edge erosion in turbomachinery and rotorcraft. For turbofans the issue is twofold: buzz saw noise produced at take-off and broad band fan noise. Leading edge erosion also increases the risk of unstable vibrations ('blade flutter').

To control roughness and profile form of the leading edge, technologies such as surface engineering are used. Such solutions involve functionally graded surfaces or coatings to protect the leading edge. Other technologies such as flow control methods, either passive [6] or active [7], are also being investigated to improve the aerodynamic performance of wind turbine aerofoils that suffer increased surface roughness. A passive flow control device, termed as leading edge protuberance, has gained attention [8] in recent years. There is research that shows that leading edge protuberances can significantly improve the aerodynamic performance [9-11]. Such designs are based on biomimetic approaches such as Fish et al. [12-14] who found that humpback whales with a tubercled pectoral flipper became highly maneuverable while Miklosovic et al. [15] show that the tubercles on the pectoral flipper model can increase the stall angle and also achieve a higher lift coefficient and a lower drag coefficient at larger attack angles. Considerable research is now focused on leading edge protuberances, as a passive control method to improve the performance of hydrodynamic or aerodynamic bodies, such as aerofoils, wind turbine blades, propellers, rudders, and hydrofoils [16].

As discussed above the efficient working of the turbine stage of an aeroengine depends on the kinematics and dynamics of fluid flow through the channels between the blades. Conversion of energy from one form to another and its efficiency in each turbine stage depends, among other things, on the roughness and geometric shape of blades.

With the development of detection and sensing technology, fast and accurate inspection of the leading edge of turbine blades has become possible. The geometric accuracy of these blades can be verified using both contact coordinate measuring machines (CMM) [17-19] for objects with free-form surfaces [20, 21], and non-contact coordinate measuring methods using measuring arms [17, 22], as well as phase measurement profilometry [23]. The selection of a suitable probe radius correction method for coordinate measurements that can be applied to turbine blades is presented by Kawaleo et al [24] based on Bézier curves. Recently, computer vision has been used to detect damage features in images of the leading edge taken by cameras carried by drones which were stitched together to produce 3D reconstructions [25]. This process is also referred to as "Structure in Motion" (SfM) [26], which is useful for large-scale or applications in difficult-to-access locations such as wind turbines. It should be noted that most of the measurement systems are for form only and cannot obtain roughness/features at the micrometer level. Where surface roughness evaluation is critical, replicas or portable surface roughness devices can be used for these more detailed surface topography measurements.

Therefore, the scope of this review paper will focus on the topography induced by material responses and propagation of roughness to leading edges of turbomachinery blades. The paper is structured in two parts 1) additive/subtractive processes and the effect of this roughness change on performance and efforts to predict and model these changes; and 2) applications mainly focused on turbofan engines, gas and steam turbines, wind turbines, marine current turbines and marine propellers. Therefore, this paper has not included roughness / texturing effects of other parts of the blade.

2. Processes that effect roughness of leading edges

2.1. Additive processes

The additive process is caused by the adherence of dirt to blades/ aerofoils surfaces, especially around the leading edges. Insects, icing and particles like smoke, oil mists, carbon, and sea salts are most typical examples [27]. Due to the accumulation of contaminants on the leading edge of the blades/ aerofoils, the build-up of material leads to an increase in surface roughness and to some extent alters the shape of the aerofoil (if the material builds up to form a thicker deposition layer). As a results of the increased roughness, significant losses in power output and stall behaviour have been reported for wind turbines [28] and marine current turbines [29], and performance deterioration for compressor rotor [27].

2.1.1.Icing

Turbomachinery operating in cold regions or at high altitudes often face icing problems, especially during winter operation. The most typical atmospheric icing types are in-cloud, precipitation and frost icing [30-32].

In-cloud icing occurs when supercooled water droplets hit a surface below 0℃ and freeze on impact. The droplet temperature can be as low as -30℃, but due to their size, they do not freeze in air. Accretion of ice exhibits different sizes, shapes and properties based on the number of water droplets in the air (liquid water content - LWC) and their size (median volume diameter - MVD), temperature, wind speed, duration and collection efficiency. The density of accreted ice ranges from low (soft rime) over medium (hard rime) to high (glaze). Soft rime is represented by thin ice with needle and flake shapes. This type of icing with low density and low adhesion occurs when the temperature is far below 0℃ together with low LWC and MVD. The hard rime formed under higher MVD and LWC conditions has a higher density and is more difficult to remove. Glazing occurs when a portion of a droplet does not freeze on impact, instead they flow across the surface and subsequently freeze. It is usually associated with precipitation and results in a very dense and adherent glaze [33]. The types of in-cloud icing as a function of wind speed and air temperature are shown in Figure 3.

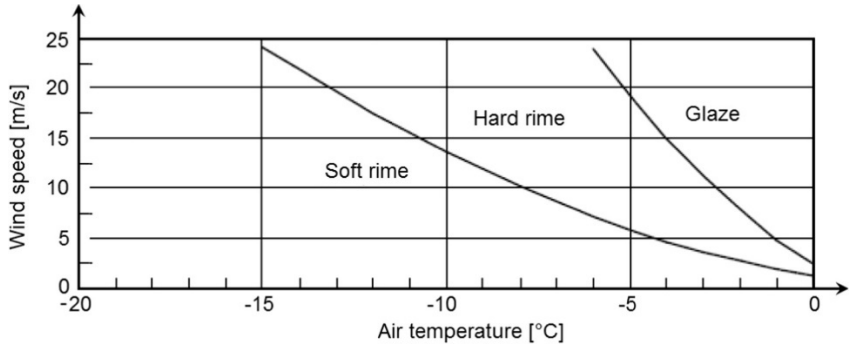

Figure 3 Type of in-cloud icing as a function of wind speed and air temperature [34]

Precipitation icing can result from wet snow or freezing rain, which may accrete at a much higher rate and cause more damage than in-cloud icing. Wet snow refers to slightly liquid snow at air temperature between 0℃ to -3℃. Removing wet snow from the surface is easy, but removal will become very difficult when the surface is frozen. Icing from freezing rain often occurs during inversion, when rain falls on a surface at a temperature below 0℃. Both the density and adhesion are high with this type of icing. Frost occurs when water vapor cures directly on a cool surface. It often occurs during light winds, and the adhesion can be very strong. An example of icing on a wind turbine blade are show in Figure 4 and Figure 5.

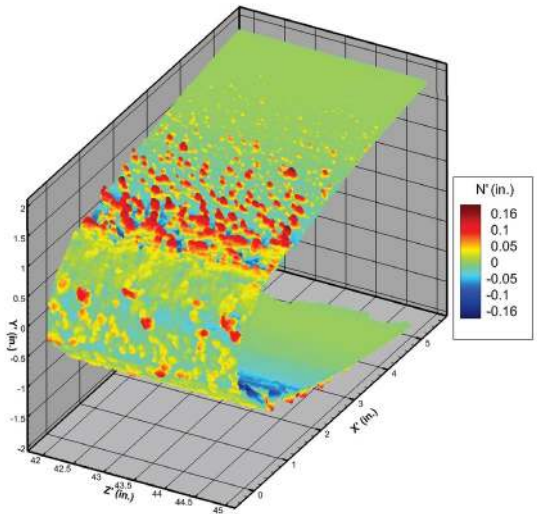

Figure 4 Roughness visualization of the 031414.01 ice surface [35]

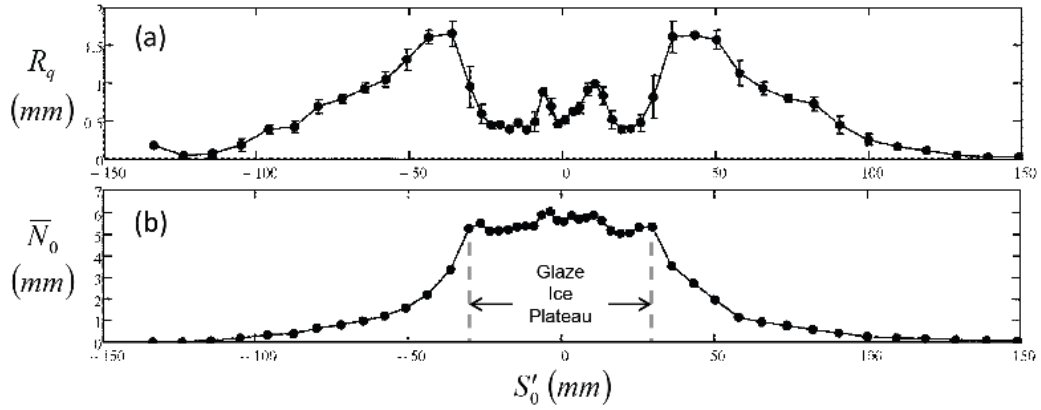

Figure 5 Reduced roughness (a) and thickness (b) variations along the 031414.01 ice surface [35]

2.1.2.Insects

Early studies of atmospheric insect populations were conducted to sample and identify flying insect species in the 100m above ground region of southern Great Britain [36]. The most prominent species found under these conditions were aphids and drosophila melanogaster, commonly known as the fruit fly. Lift and drag coefficients of the wings of such insects along with insect rupture velocity (V_{rup} = 10.8 m/s) were estimated by later aerodynamic studies [37, 38]. According to a recent study by Voigt, a single turbine located in the temperate zone of Germany might kill about 40 million insects per year [39]. However, studies of insect populations worldwide and at various altitudes have not been extensively reported in entomological literature [40].

Insects prefer to fly in conditions of high air humidity, low wind speed and temperatures above about 10℃ [41]. In these conditions, numerous insects impact wind turbine blade leading edges, streaks of liquid and the remnants of crushed insect bodies adhere to the surface of the blade surface, resulting in increased roughness. Insect roughness is considered to be randomly distributed roughness and usually affects blades within the first 15% of the chord [42]. Insect roughness appears heavily depend on the rain frequency, that extreme insect roughness in Figure 6 (a) was captured after four dry months, whereas the sparse insect roughness in Figure 6 (b) was observed after one rainy month (5.4 in of rain) [42].

(a) (b)

Figure 6 Images of insect roughness on leading edges. (a) Heavy insect roughness from Spruce [43, 44] and (b) minimal insect accumulation from Ehrmann [42]

According to Coleman [45], a low estimate for the height of excrescences left by fruit flies or house flies is around $330\mu m$. While the maximum height from large or accumulated insects could reach $750\mu m$ to $1370\mu m$ for different turbines [45, 46]. The boundary layer is negatively affected by the increased roughness, that local flow separation and transition from laminar to turbulent may occur, if the residual debris thickness exceeds the boundary layer critical height [47]. Another experimental study found the surface roughness has a significant influence on the amount of haemolymph from spreading on surface after impact, and that rough coated surfaces (Ra = 4.91 μm and 5.26 μm) showed less effective adhesion compared to the smoother coated surface (Ra = 0.24 μm) [48].

2.1.3.Marine biofouling

Marine fouling is the accumulation of microorganisms and microbes on submerged surfaces, leading to negative impacts in economic, environmental or safety-related issues. Surface roughness generated by marine fouling will increases the drag resistance and poses a performance risk to any long-term marine application whose performance depends on boundary layer hydrodynamics (e.g., vessel drag) [49]. It is a worldwide problem in marine systems, costing the US Navy alone an estimated $1 billion a year [50]. According to [51], more than 4000 species of fouling organisms have been identified worldwide. Of these, barnacles are one of the main sources of macro-organisms and probably also the one that causes the most problems. Once they seize the opportunity to attach to the hull of a ship or any other surface in the marine environment, they form a calcareous matrix wall around their soft body (shell) [52].

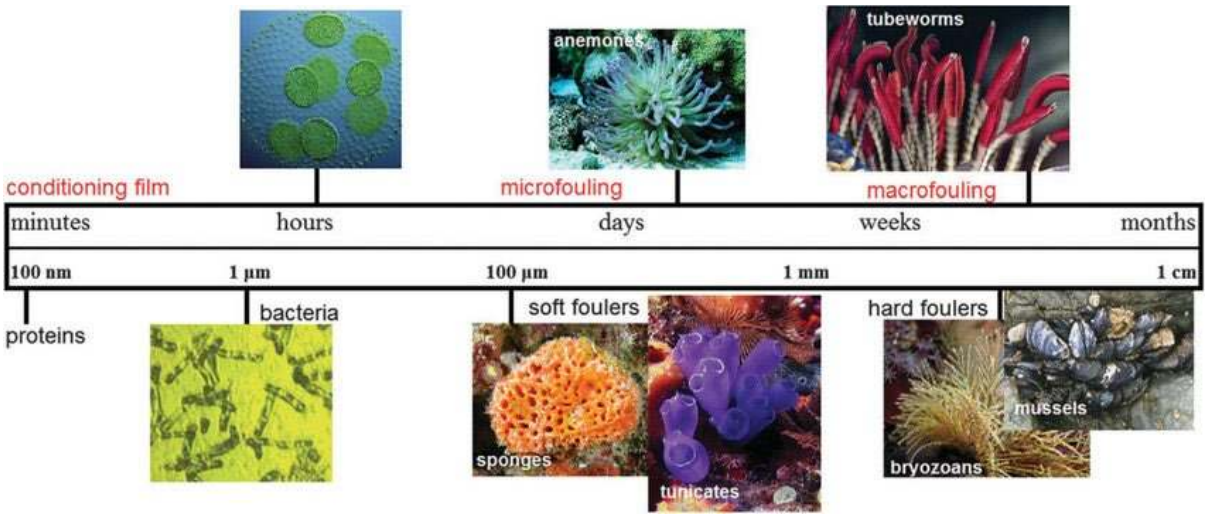

Figure 7 Different phases of marine biofouling: Time-line evolution and respective roughness increase [53]

The evolution of marine biofouling organisms and changes in their morphology and size over time are shown in Figure 7. Biofouling of turbine rotor blades increases the surface roughness, and the increased roughness will alter the flow field near the blade surface (i.e., the boundary layer). At moderate to high Reynolds numbers, increased surface roughness decreases lift and increases drag, thus reducing time-averaged hydrodynamic torque on the rotor [54]. The magnitude of this reduction depends on the roughness height, chord position, fouling density and aerofoil shape. Surface roughness increases mixing in the boundary layer and may lead to earlier and longer turbulence transitions along the aerofoil [55]. In addition, as the roughness height increases, the viscous resistance increases due to the higher local velocity shear rate of the blade surface [54]. Impact of biofouling on turbine hydrodynamics depends on the species composition and maturity. Even biofilms as thin as 0.1 mm have been shown to increase skin friction on flat plates [56], while the barnacle heights can exceed 10 mm [57]. Barnacles at such size would cause local flow separation on the turbine blades and thus affect lift and drag components, and even lead to dynamic stall [49].

2.1.4.Particle attachment

The particles that cause fouling are usually in the range of 2 to 10 μm, and the most typical examples are smoke, oil mist, carbon, sand, volcanic ash and sea salt etc. The particle attachment involved in turbomachinery is a two-step process: delivery of particles to turbine surface and particle deposition (attachment). Fouling can be controlled by a suitable air filtration system, and it can usually be reversed to some extent by washing the components with detergent. The adhesion of the particles is impacted by oil or water mist [27], and higher temperatures can negatively affect the deposition problem by increasing the stickiness of the particles [58].

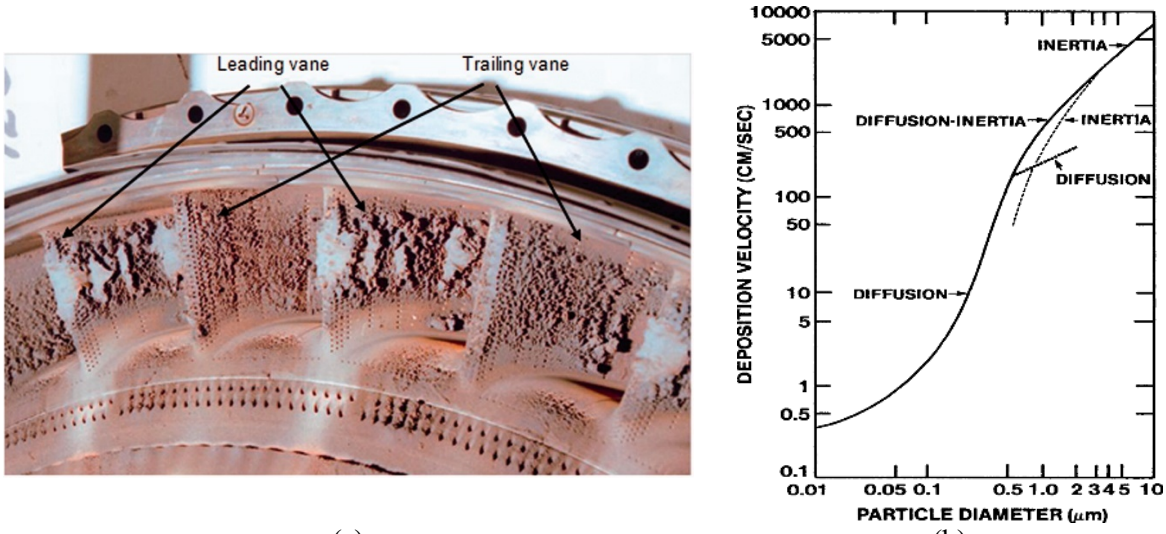

(a) (b)

Figure 8 (a) Volcanic ash deposition on turbine vanes [59] and (b) Turbine vane deposition vs particle diameter [60]

Particle clouds from volcanic eruptions are one of the most dangerous environments for aircraft engines, and several incidents were found related to engine operations in volcanic ash cloud environments. An example of dust and volcanic ash deposition on the high-pressure turbine vanes is shown in Figure 8 (a), and the effect of particle diameter on deposition velocity (deposition rate normalized to airflow particle concentration) is illustrated in Figure 8 (b). The deposition velocity was calculated from particle delivery model that utilise the concave (pressure) surface at trailing edge of the first stator vanes in large utility turbine [60].

2.2. Subtractive processes

The word "erosion" is from the Greek word "erodere" and is defined as surface destruction and material removal by external mechanical forces of multiple impacts generated by dynamic impingements of a liquid on a solid surface (cavitation erosion and water droplet erosion) or of a solid on another solid surface (solid particle erosion). Therefore, there are two types or erosion, namely solid erosion and fluid erosion [61]. We have included foreign object damage (FOD) as a subtractive process and will treat it as an extreme erosive process, although it may not lead to material loss itself, it does lead to lower erosion and component level fatigue resistance. Oxidation, a subtractive process, of the blade materials induced by the high temperature environment has not be found to be a predominant mechanism for influencing leading edge roughness, so is not included in the following sections.

2.2.1. Solid particle erosion (SPE)

For SPE, the influential factors are angle of incidence or impingement angle of particles, size, density, shape and velocity of particles and number of impingements. Particle impingement can cause cutting, plastic deformation or brittle fracture on the surface as well as large-scale subsurface deformations, crack initiation and propagation as well as subsequent material ejection.

SPE can result from fine particle ingestion into turbomachines, such as gas turbine engines as well as centrifugal and axial compressors, [62]. Aeroengines operating in dusty environments are subjected to ingestion of erodent particles leading to solid particle erosion (SPE) of engine blades and a subsequent drop in aerodynamic engine performance [63]. SPE in aeroengines can take place when the plane takes off from a sand-covered runway or at high altitudes where it encounters hail, sand or volcanic ash. SPE can also be accompanied by water droplet erosion (WDE).

2.2.2. Water droplet erosion (WDE)

Water Droplet Erosion (WDE) is defined as the “progressive loss of original material from a solid surface due to continued exposure to impacts by liquid drops or jets” [64]; where, in this case, the liquid is restricted to water and the form restricted to drops. A significant range of detrimental material responses are generated by repeated droplet impingement. These include fracture-based mechanisms of in brittle materials, to unusual ‘fatigue-like’ behaviour and pitting in ductile metals. The response of material is often greatly influenced by the ‘severity’ of the repeated impingements, and the impingement velocity provides a good indicator of severity [65]. The physics of the droplet impingement is such that kinetic energy is not a good indicator of erosion severity unlike SPE.

Rain erosion, or WDE, of turbofan blades, has been of growing interest to the aeronautics community recently [66]. This phenomenon leads directly to the loss of thrust and a decline in engine performance and increases the risk of flutter [65, 67]. WDE is also commonly seen in steam turbine and wind turbine blades, as shown in Figure 9. Over a number of cycles, the leading edge is roughened and their profile (form) changed. For steam turbine, WDE shortens the chord length of the blades, resulting in a larger gap between the trailing edge of the blades and the turbine housing, and a consequent reduction in the output energy and overall efficiency of the turbine.

WDE can clean away the additive processes mentioned above, i.e. insect, particle attachment. This leads to an antagonistic process and smoothing of the surface where WDE interactions with SPE can lead to synergistic processes and increase roughness and material removal.

(a) (b)

Figure 9 Water droplet erosion at the leading edge of the steam turbine blade [68]; (b) wide areas of erosion of wind turbine blade [69].

2.2.1.Cavitation erosion (CE)

During the CE process, microjets at 200-300 ms^{-1} are formed by asymmetric implosion of cavitation bubbles on to a solid surface, generating high impact pressure (albeit on a smaller scale areas (tens of μm) compared to droplet impacts (hundreds of μm)) and stress waves [70]. The performance of materials shows similarity under the WDE and CE tests and CE is proposed as a screening process for WDE [71, 72]. Cavitation is usually defined as the generation of cavities and the subsequent dynamic behaviours that occurs when a liquid is subjected to a sufficient pressure drop [73]. It has been widely used in sonochemistry, biomedical, environmental science and many other fields [74] due to the high temperature and pressure [75, 76], light emission [77], shock wave [78], micro jet [79] and the resulting biochemical effects [80] caused by cavitation bubbles. However, cavitation erosion is also a major failure mechanism for many fluid machinery components. In a recent paper [81], the influencing factors of ultrasonically induced cavitation intensity are found to be complex and related to the surrounding liquid environment, ultrasonic frequency and pressure and bubble size.

2.2.2.Foreign object damage (FOD)

Foreign object debris refers to any object located in and around an airport (especially on the runway and the taxiway) that can damage the aircraft or harm air-carrier personnel [82]. The most common foreign object debris examples include twisted metal strips, stones, components and plastic products detached from aircraft or vehicles. Foreign object debris can pose safety risks to aircraft and significant economic losses to airlines [83]. In 2009, the well-known incident of US Airways flight 1549 that loss thrust in both engines was caused by a flock of Canada geese. Moreover, the direct economic loss due to foreign object damage (FOD) is conservatively estimated to be 3 ~ 4 billion USD per year [83, 84]. As suggested by [85], FOD is a prime cause for maintenance and repair in aircraft engines due to its influence on the high-cycle fatigue properties of key engine components. Bird strikes are the most common cause of in-flight FOD and turbofan engines experience more severe FOD incidents on the ground than in-flight condition.

For rotor machinery elements, FOD induced by hard body impacting on fan blades can result in immediate blade fracture or damage from stress-raising notches [86, 87] or cracks [88], significant deformation and even loss of complete blades. In a recent study on Ti6Al4V alloy [88], where FOD was simulated by high-velocity impacts of steel shot on a flat surface, a fatigue life reduction was reported and associated with microcracks generated in the pile-up of material around the impact crater rim, which act as preferred sites for the premature initiation of fatigue cracks. Peters et al. [88] found that crack initiation in the vicinity of FOD occurs at cycle lifetimes that are orders of magnitude lower than found for un-impacted specimens. High-speed impacts were also observed to have caused micro-structural distortion, in the form of shear bands formatted at crater rim by 300 m/s impacts, although it

was not evident that they had any effect on the fatigue life. Shear bands were not observed for lower-speed impacts.

Other work has looked at the damage from high-speed cubes impacting the leading edge of aerofoil specimens. This type of FOD can be characterized as a combination of notch indentation, material loss, material shearing, material folding, heat formation, shear bands and microcracks. All of those characteristics can lead to material fatigue and thus reduce the overall performance of the blade [89]. An experimental study of high velocity oblique impact on carbon/ epoxy laminates was conducted by Kristnama, and Figure 10 present the CT scan of the post-impact damages for edge impacted laminates at 200m/s and 350m/s [90]. As the impact angle of the foreign object varies, its influence on the fatigue performance of the blade are also different. Moreover, the residual stress caused by the FOD can also adversely affect the fatigue performance of blades [91].

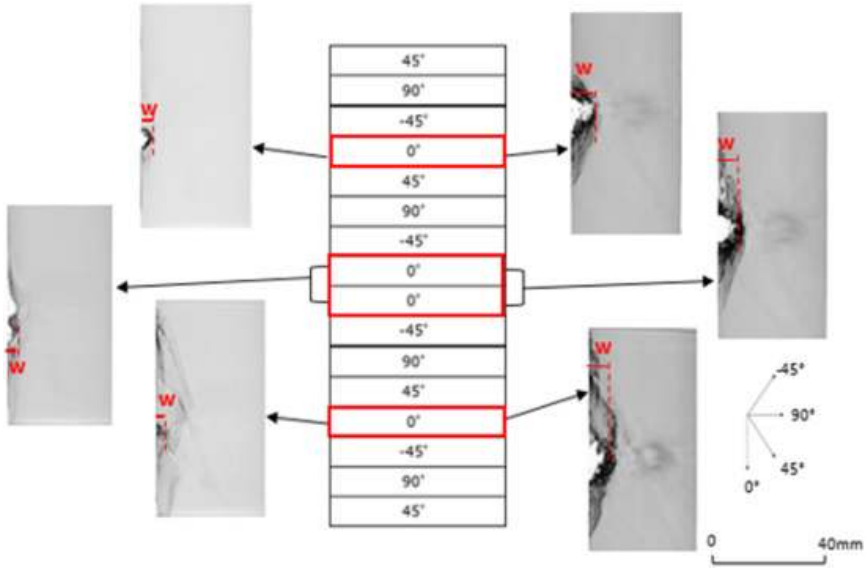

Figure 10 Fibre fracture width definition for edge impacted laminates at impact velocities 200 m/s (left) and 350 m/s (right) [90]

3. Turbofan engines

Modern aircraft normally use turbofan engines due to the advantages of high thrust and fuel efficiency when compared to propellers. A turbofan engine generally consists of four sections: the fan, the compressor, the combustor and the turbine; see Figure 11. At the front end of the engine, a fan helps to increase the ambient air flow into the compressor. The compressor, which includes intermediate pressure compressor (IPC) and high pressure compressor (HPC), pressurises the air flowing through the engine before it enters the combustion chamber. The air is then mixed with fuel, ignited and burnt in the combustion chamber. The last stage is the turbine, which extracts work from the high-pressure hot gases exhausted from the combustion system, and powers the compressor stages and auxiliary engine systems.

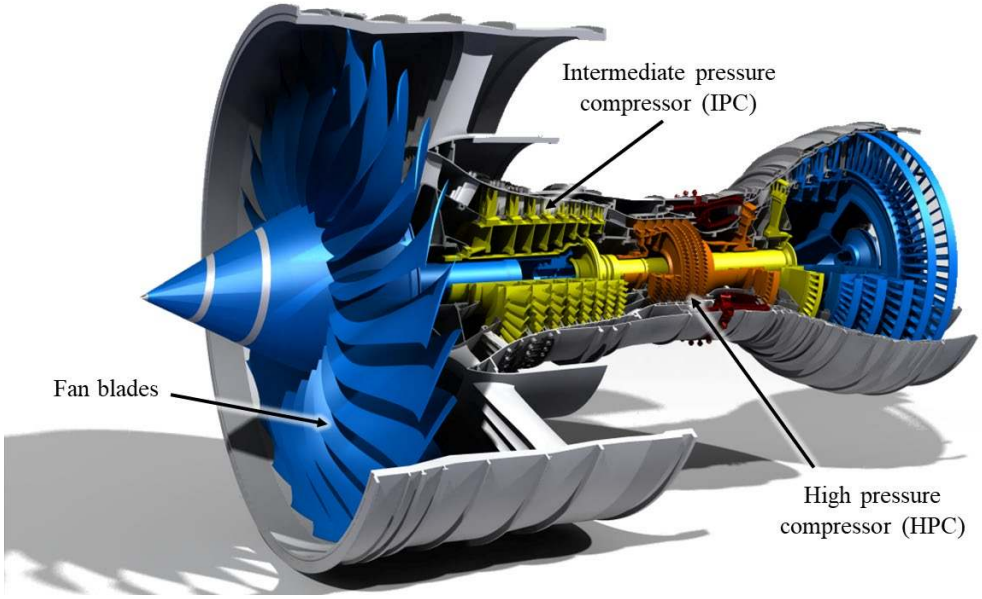

Figure 11 Cutaway view of the Rolls-Royce Trent 900 turbofan engine [92]

The operation of modern gas turbines demands ever higher temperatures, pressures and rotational speeds to increase power and efficiency [93]. This ultimately creates a tough environment for engine parts, especially engine blades. These blades are subjected to extreme operating conditions, such as high centrifugal loads, heat, high pressure and vibration [94-97]. Therefore, the manufacture of turbofans employs a range of lightweight, high-strength, corrosion resistant and thermally stable materials. Typically, Titanium alloys are used for the blade material in the fan and compressor sections of the engine, but more recently composite fan blades with titanium shielding at the leading edge have been applied in some turbofan engines. Besides, aircraft engine maintenance is complex, time-consuming, expensive, and has a significant impact on function and safety. Engine blades and vanes are the least qualified parts during engine maintenance. As a result, there is an ongoing need for more efficient inspection procedures [98].

3.1. Intake fan blade

As mentioned above, turbofan blades suffer from various FOD by debris of aircraft parts or external objects, such as volcanic ash, sand, bird strikes or harsh weather conditions (rain, fog or hail) as well as salt spray [99] and organic material [100]. Failures of turbofan blades can affect the thrust generation and eventually resulting in the efficiency drop of the aeroengine [101-103]. The intake fan blades must be able to avoid fracture when birds and other debris are sucked into the engine and strike its blades. Compressor blades can be subjected to the foreign particulate impacts listed above and domestic impacts such as oil droplets and rotor path material, and these have a detrimental effect on compressor efficiency by way of deposition or SPE of gas flow path surfaces.

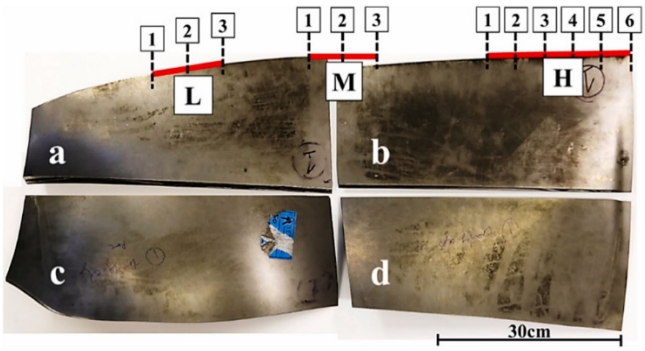

Figure 12 ex-service turbofan blade [104]

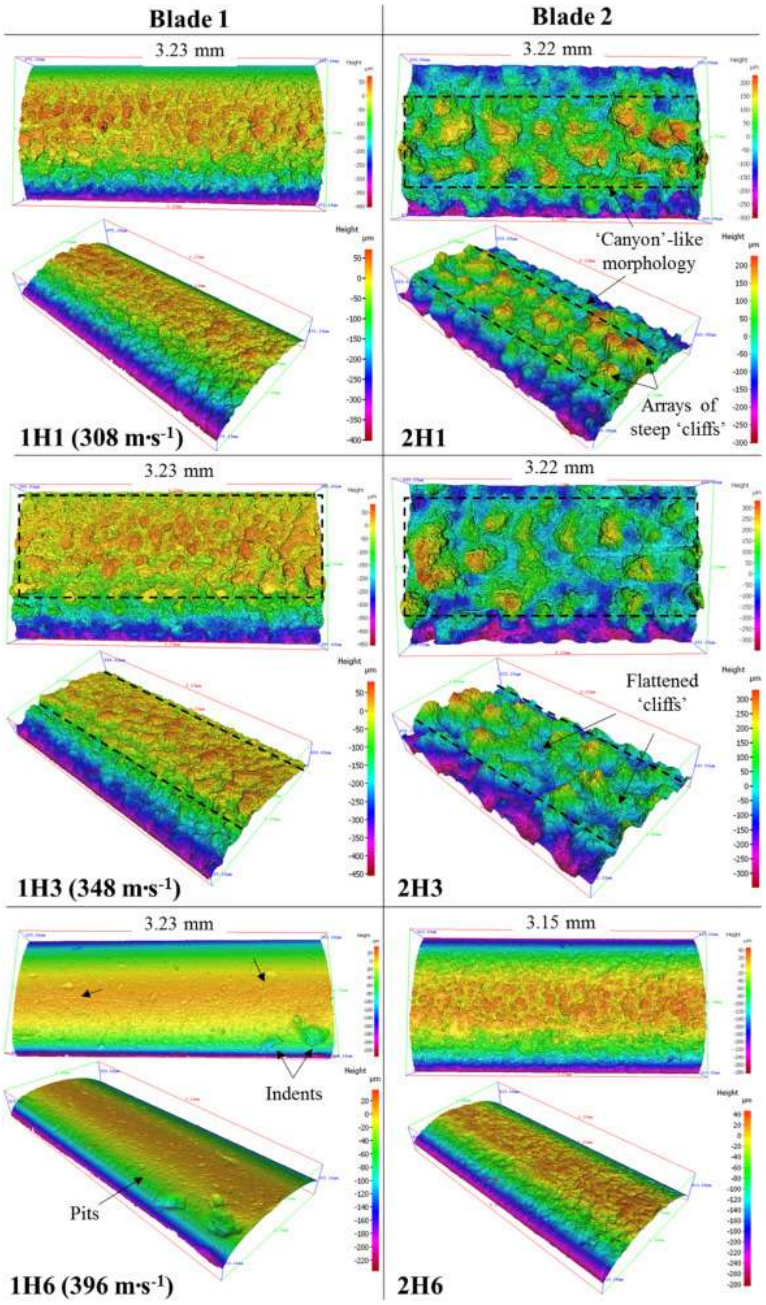

Figure 13 3D profiles of H1, H3 and H6 zones of both leading edges [104]

Ma et al [104] produced a forensic analysis of rain erosion damage of the leading edges of two ex-service Ti-6Al-4V fan blades from different aeroengines with respect to the microstructure, morphology and impact conditions to examine the WDE damage mechanisms on the leading edges and their evolution This work shows the rain erosion process develops with increasing impact velocity, see Figure 13. At M (moderate speed) and H (high speed) zones, shown in Figure 12, 'canyon'-like morphology starts to form on both blades due to significantly increased material loss. However, more prominent 'canyon' features are observed on Blade 2 leading edge with steeper 'peaks' and deeper 'valleys', as shown in Figure 13 - 2H1 and 2H3. The severity of the rain erosion damage decreases after the H3 zone towards the tip of the blade (H6 zone) at both leading edges. This is attributable to the shielding effect of the fan blade casing and flow field at the blade tip. The impact velocity was assumed to be

proportional to the blade radius. Hence, the corresponding impact velocity for each site of the leading edges is computed and listed in Table 1 .

Table 1 Impact of velocity at each site of the leading edges [104]

Impact velocity / m·s^{-1}											
Root side				Centre				Tip side			
L1	L2	L3	M1	M2	M3	H1	H2	H3	H4	H5	H6
144	164	204	226	246	286	308	328	348	368	382	396

More significant increase of WDE damage was observed in the velocity range of 286 m s^{-1} to 348 m s^{-1}.

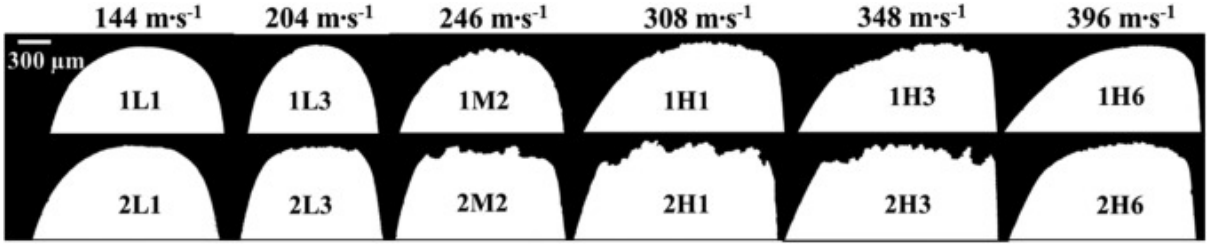

Figure 14 Comparison of cross-sectional profiles of ex-service turbofan leading edges [104]

More significant increase of WDE damage was observed in the velocity range of 286 m s^{-1} to 348 m s^{-1}. The relationship between volume loss and linear velocity for this velocity range was found to be:

$$\frac{v_2}{v_1} \propto \left(\frac{V_2}{V_1}\right)^{8.15} \tag{1}$$

where υ is the relative volume loss and V is impact velocity. The erosion volume loss exhibits significant sensitivity to the impact velocity, that the erosion volume loss is found to be proportional to the 8.15 powers on impact velocity.

Cross-sectional observations on the leading edge specimens shown in Figure 14 can further verify the relation shown in Eq. (1). Comparison of Blade 1 and Blade 2 cross-sections reveals that the rain erosion damage initiates at the highest curvature of the leading edge profile, as shown in Figure 14- 2L1. The affected zone is then expanded with increasing impact velocity. The severity of material removal increases significantly for impact velocity over 246 m s^{-1}. The whole tip of the leading edge was removed in 2M2, 2H1 and 2H3. The paper summarises the development of roughness and flattening of the leading edge using Figure 15. This schematic figure was informed by multiple cross-sections and SEM analysis of the damaged blade at multiple locations on each blade.

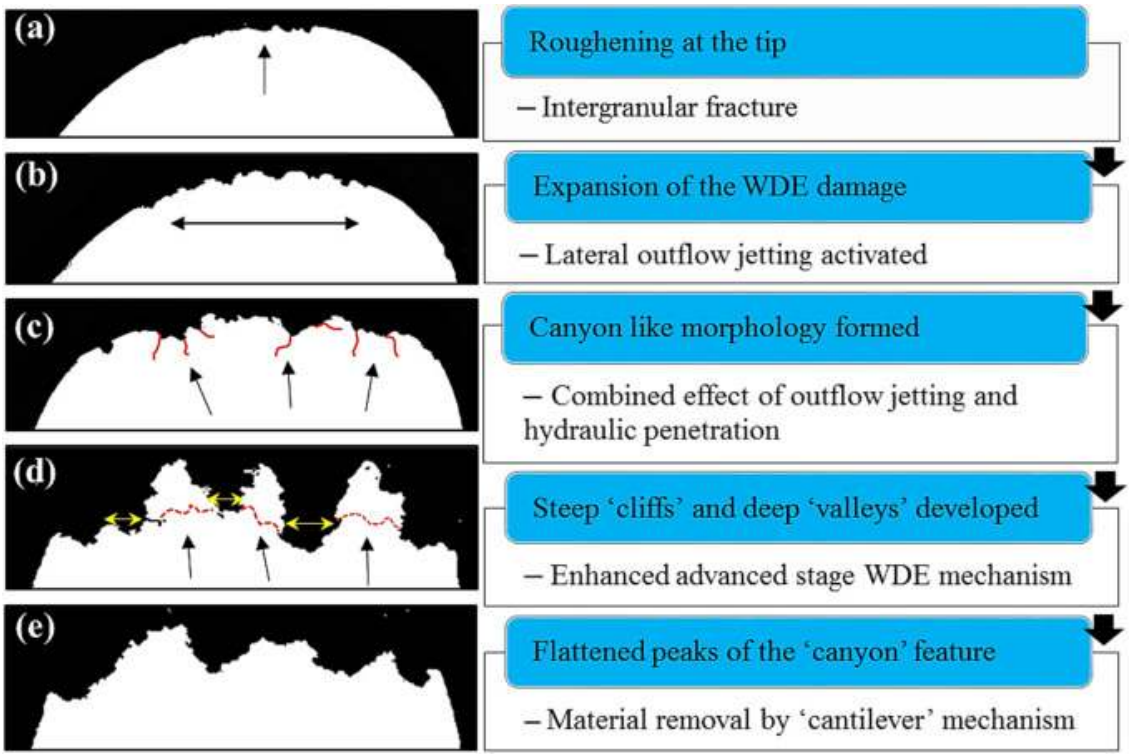

Figure 15 Evolution of rain erosion at the leading edge of Ti-6Al-4V turbofan blades [104]

The evolution of rain erosion at the leading edge of Ti-6Al-4V turbofan blades is demonstrated with a series of cross-sectional blade profiles shown in Figure 15.

a) The initiation of rain erosion occurs at the highest curvature of the leading edge profile. The intergranular fracture observed in the early stages of WDE can be attributed to the high anisotropic behaviour of α-grains in Ti-6Al-4V blade material under water-hammer pressure.
b) Followed by the initial short and high pressure compressible stage of impact, the shear stress due to the activation of the lateral outflow jetting leads to the formation of cracks and erosion craters. Subsequently, the WDE damage area expands.
c) Erosion craters are broadened and deepened by a combination effect of lateral outflow jetting and hydraulic penetration, resulting in a 'canyon'-like morphology at the leading edge surface.
d) Such mechanism is aggravated by the droplets impinging at over 246 m s^{-1}, and the increased maximum erosion rate fashions the 'canyon' with steep sides 'cliffs' and deep 'valleys', as well as re-entrant features that exhibit a finger-like cross-section.
e) The 'peaks' of the 'canyon' are eventually removed by the 'cantilever' mechanism.

It was found that the primary mechanism for material removal in the advanced stages of rain droplets erosion at supersonic impact velocity is the process of hydraulic penetration (tunneling, and upheaval of the overlying materials) due to the effect induced by repetitive droplet impingements. The presence of nano-size cavities observed at the leading edge of the ex-service fan blade indicates the action of hydraulic penetration. Cavities of this nano scale have not been reported in laboratory based WDE studies to date [104, 105], which might suggest slight differences in droplet / solid behaviour in service.

3.2. Compressor blade

The degradation of the leading edge of a compressor blade in an aircraft engine during service has a disproportionate effect on compressor efficiency. Wilshee [106] tested compressor blades with roughness imposed onto discrete regions and found that applying roughness over the leading edge and the first 4% of the chord (for blade nomenclature see Figure 16) increased the aerodynamic losses by

approximately a half of that observed when the entire blade was roughened. This is attributed to the boundary layer around the leading edge being much smaller and the roughness, therefore, will have a larger effect. Goodhand and Miller [107] tested compressor blade with different leading edges to demonstrate their sensitivity to blade geometry. They found that premature flow turbulence and associated losses caused by circular leading edges could be offset by a 3:1 elliptical leading edge. Similar or even larger changes to leading geometry may occur in service due to either additive or subtractive processes (i.e. erosion or deposition) [108].

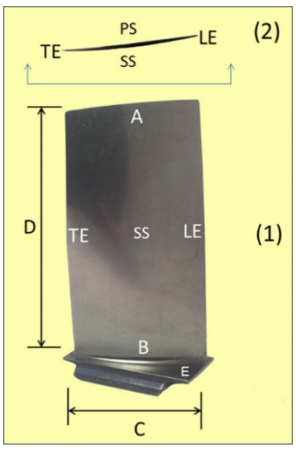

Figure 16 Generic compressor blade nomenclature; (1)-side view and (2)-tip view(x section) showing; LE-leading edge, A-tip, B-root, C-chord (chordwise direction), TE-trailing edge, D-Span (spanwise direction), SS-suction side (convex), PS-pressure side (concave), E-end wall [108].

Walton et al [108] presented a study that focused on the leading edges of the rotor blades from a single engine; measurements were taken from one blade from each row of the IPC and one from each row of the HPC. This allowed him to study leading edge of different sizes as well as different levels of degradation. Walton detailed an automated technique for roughness of the leading edge characterisation in terms of areal parameters and the spatial distribution of peaks in this characteristic roughness.

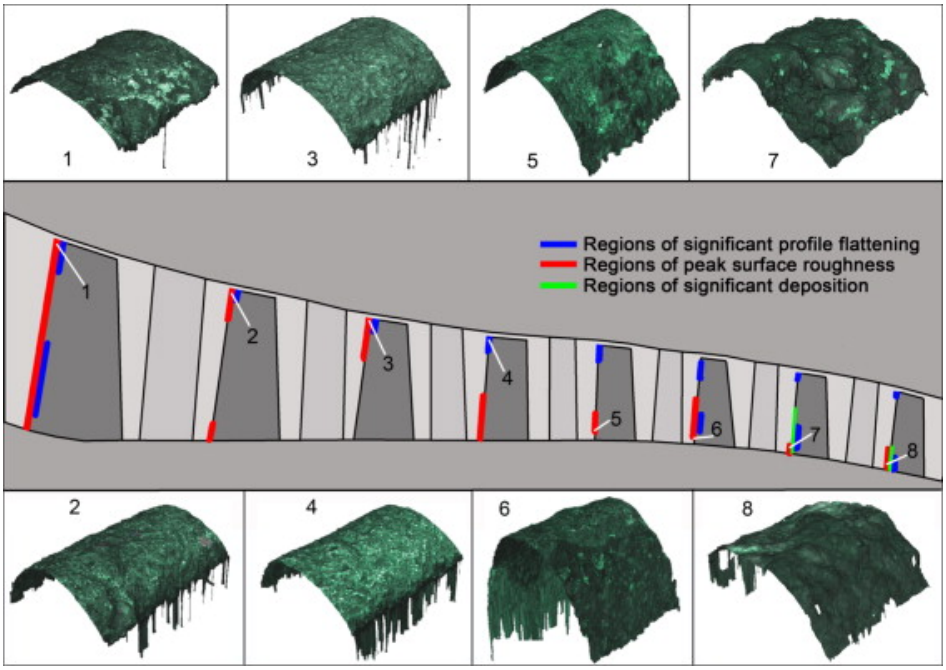

Figure 17 Schematic annulus diagram of the IPC showing blade number. In red are regions of peak surface roughness. In blue are regions of (relative) pronounced increase of fitted radius due to erosion of profile. Above and below are leading edge fields from the numbered blades in the LE positions indicated by the white lines [108]

Figure 17 shows the spatial distribution details of leading edge peak roughness of the IPC, as well as regions of profile flattening (increased fitted radius) due to erosion of the leading edge. Walton presented a single field image for each blade to illustrate typical features of the surface character and geometry. IPC1 is seen to show essentially uniform roughness with the highest mean value in the IPC only exceeded in the compressor as a whole by that of HPC2. This pattern was attributed to particulates entering the compressor that have not yet been subjected to any significant fragmentary or centrifugal action, and were therefore relatively large and uniformly distributed. Before the start of deposition at IPC7 (see Figure 17), only the effects of erosion were characterised in the results. This work concluded that spatial characterisations could indicate the leading edge regions that are most susceptible to in-service damage and, therefore, useful to inform designers on locations to consider applying coatings. In addition, they show that peak wear and roughness are not uniformly correlated. The authors also state, uncertainty remains as to the length scale at which degradation features should be segregated for characterisation as changes in geometry or surface roughness [108].

A recent paper, has investigated the surface roughness of rotor blades of a compressor from different stages of an axial high-pressure compressor and a first stage BLISK (Blade–Integrated–dISK) of a regional aircraft engine, see Figure 18. Measurements by a three-dimensional laser scanning microscope found the largest roughness height in the first stage followed by the centre stage and the last stage of the compressor. Basic types of roughness structures were identified as impacts as round depressions of different sizes, depositions isotropically distributed single elements with steep flanks in different size and anisotropic roughness structures. Although the anisotropic structures can only be detected at the leading edge of a single blade in the first stage of a medium-sized engine. These structures are oriented at an angle ranging from 45° to 90° normal to the flow direction and are the result of leakage oil and flow particles. These structures lead to a higher equivalent sand grain roughness (k_s) magnitude, which is not detectable in the standard roughness parameters (*Ra*, *Rq* and *Rz*). On the pressure side, the highest roughness is detected at the leading edge, identified as a mix of erosion, impacts and depositions [109].

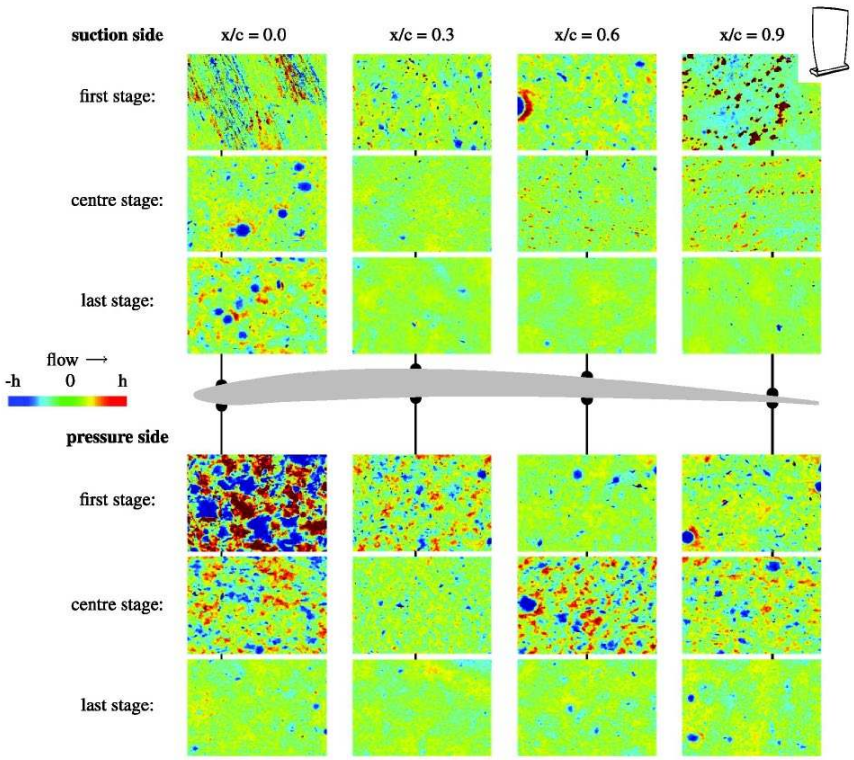

Figure 18 Examples of single-blade roughnesses from a high-pressure compressor of a mid-size aircraft engine from different stages and measurement positions. The size of the measurement area is 0.890 mm by 1.280 mm [109].

Compressor rotor degradation caused by fouling (adherence of particulates) has been extensively investigated and recently reviewed [27]. The authors noted that fouling is primarily the result of deposition of 10 μm to sub-micron sized particles by a diffusion mechanism, with smaller particles in that range predominating the process. The wetness of particles or surfaces increases the probability and possible size of particle adhesion. In addition, the elevated temperature seen in the HPC is considered to increase the stickiness and thus the probability of particulates adhesion. Fouling degradation provides the opportunity for partially or fully recovery of surface integrity through detergent washing, as documented by [99, 110].

Helicopter engines suffer blade roughening and damage (SPE), particularly in sandy environments. For example, in the first Gulf War, the severity of damage to unprotected Chinook engines led to rejection rates of 20 to 40 engines per 1000 flight hours. Compressor blades are more severely affected by hard quartz particle damages, with blunted leading and trailing edges and pitted pressure surfaces. While the turbine blades are subject to heavy accumulation of molten deposits due to impurities solidifying on film cooled surfaces [111].

3.3. Repair and protection strategies

Leading edge repair of fan and compressor blades can include blending of the leading edges, profile re-contouring by adaptive milling, salvaging FOD blade by hot forming and patch repair, repair with EB welded inserts [112].

Fan blade protection is used where economically beneficial. One example is the so called BlackGold® coating (multilayered PVD nanostructured coating) being used by Delta Airlines in USA [3]. Compressor blade coatings can use PVD (Ti, Al) N or TiN (Pt) coatings (SCT 1993) or ZrN [113].

Turbine blade leading edges are equally important to engine performance. Hamed and Tabakoff presented experimental results for blade and coating material erosion showing that both erosion rate and surface roughness increase with increasing impact velocities and impingement angles of eroding particles, and larger particles produce higher surface roughness. Predictions based on the computed particle trajectories and experimental characterization of coated blade material indicates a narrow band of high erosion at the leading edge of the blade and an increase in pressure surface erosion toward the trailing edge, see Figure 19 [100].

Mechanisms of degradation and erosion of the thermal barrier coating (TBC) were reviewed by Wellman [114]. It should be noted that the TBCs on turbine blades are repairable [115], and a review of the existing techniques for removing and repairing of damaged TBC is presented by Yang [116] with the focus on the ceramic topcoats. The review shows that there is no universal method that is applicable to all coating systems. The selection of the coating removal and repair process must be specific to damaged coating systems, based on their composition, type of damage and available resources. For repair to TBCs the review shows plasma spraying or using a chemical paste are the techniques available and therefore will control the roughness of the repaired turbine blade. Blades that have been reprofiled, blended, coated, surface treated, weld overlayed or laser cladded their leading edge roughness will be determined by these processes and may well differ from the original edge roughness. Hence repaired blades will behave differently aerodynamically as well as have different mechanical properties that will affect damage tolerance and fatigue strength.

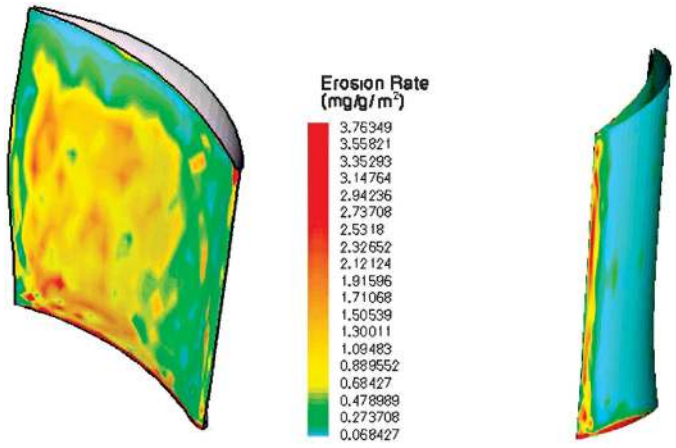

(a) (b)

Figure 19 Erosion Rate: (a) vane pressure surface and (b) vane leading edge [100]

4. Gas turbines

As mentioned in [117], WDE is also seen in compressor blades of gas turbines where the inlet air is cooled (fog cooling) to maximize air density (intake air mass) and thereby increase the power output of the turbine and the efficiency of the unit [118]. Although this method was proven to be effective, droplets are observed to cause severe damage to the leading edge of the compressor blades [119], as illustrated in Figure 20. This damage causes vibrations, which in turn increases the loss in the efficiency and results in serious fatigue damage [105].

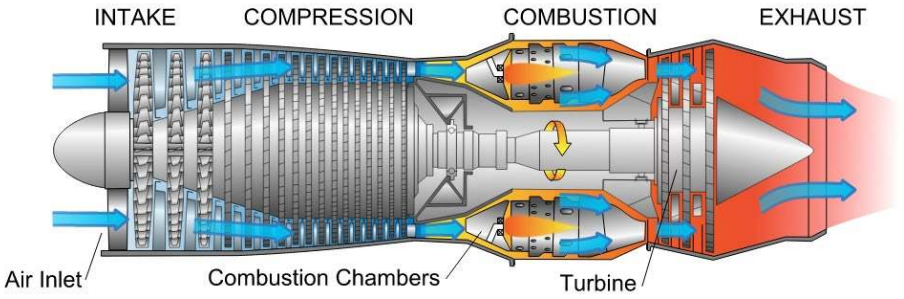

(a)

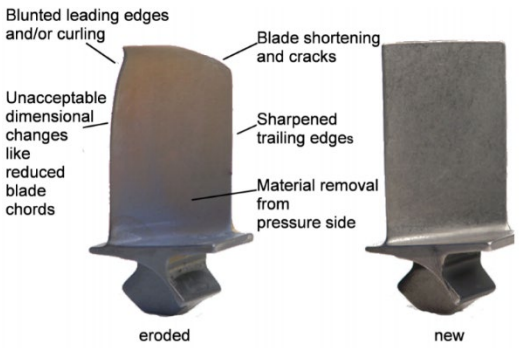

(b)

Figure 20 (a) A diagram of a gas turbine engine and (b) Comparison of eroded and new compressor blade [117]

The literature shows that the impact of whole turbine blade roughness cannot be ignored as it interacts with the boundary layer and effects aerodynamic losses. Yao et al. [120] at Tsinghua University found that the roughness effect induced by off-design incidences (i.e. deposition of the TBC) is highly

significant, but the influence of Reynolds number is less significant. Wen et al [121] indicate that rough blades change the development of vortex shedding and increase the aerodynamic loss comparing with smooth ones. However, there is limited work dealing with the effect of surface roughness on boundary layer development [122]. Bammert and Sandstede [123] show that sand grain surface roughness on the turbine blade with a roughness-to-cord ratio (Ks/C) ranging from10^{-3} to 10^{-2} can decrease stage efficiency by 7 to 14 % compared to smooth blades. Boynton et al. [124] found that decreasing the blade surface roughness from 10.2 μm to 0.76 μm causes a 2.5 % increase in efficiency of a high pressure fuel turbo pump for a rocket engine. Yun et al. [125] found that the normalized efficiency decreased by 11% with roughness of 400 μm on stator blades only, and 8% with roughness on the rotor blades only, and 19% decrease with roughness present on both the stator and rotor blades. Boyle et al [126, 127] showed that the effect of roughness on turbine blades is a function of Reynolds number. Denton [128] noted that low roughness has no effect on boundary layer at low Reynolds numbers, and aerodynamic losses become significant at high Reynolds numbers. Montis et al. [129, 130] found that with the presence of roughness on blade surface, the boundary layer upstream of the separation point will become thinner, therefore losses become significant at high Reynolds numbers. Suder et al. [131] found that the roughness distribution at the blade leading edge and in the front half of the suction surface contributed to most of the aerodynamic loss. Roughness on these regions accounted for more than 70% of the performance degradation found in fully coated blades with a surface finish of 2.5–3.2 μm (rms).

Fouling in gas turbines is caused by airborne contaminants which, under certain conditions, adhere to aerodynamic surfaces upon impact is one of the principal degradation mechanisms in the compressor section of heavy-duty gas turbines. Usually, foulants in the ppm range, not captured by the air filtration system, i.e., in the range 0–2 μm cause deposits on blading and result in severe performance drop of the compressor. Therefore, there is considerable interest in determining which areas of the compressor aerofoils are affected by these contaminants as a function of the location of the power unit. Work by Suman et al [132] looks at the estimation of the actual deposits on the blade surface in terms of location and quantity. Particle size, their concentration, and the filtration efficiency are studied to produce a realistic quantitative analysis of fouling of an axial compressor. The study combines the impact/adhesion characteristic of the particles obtained through a computational fluid dynamics (CFD) and the real size distribution of the contaminants in the air ingested by the compressor. The blade zones affected by the deposits are reported by using easy-to-use contaminant maps realized on the blade surface in terms of contaminant mass. In a more recent work, Xu proposed a model for particle deposition in flue gas turbines, and the simulation results agree with the experimental results, see Figure 21.

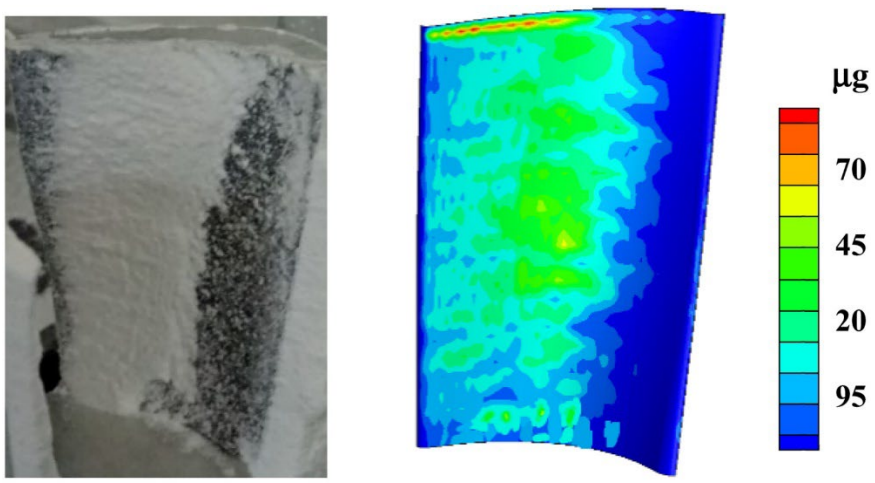

(a) (b)

Figure 21 Deposition area verification. (a) experimental, (b) simulation [133]

The analysis showed that specific fluid-dynamic phenomena such as separation, shock waves and tip leakage vortex have a strong influence on the pattern deposition. The combination of smaller particles (0.15 μm) and larger particles (1.50 μm) determined the highest amounts of deposits on the leading edge of compressor blades.

(a) (b)

Figure 22 Deposits on Low-pressure compressor (LPC) stage 2.5 blades and on High-pressure compressor (HPC) stage 3 blade [98]

The growth of these solid deposits leads to geometric changes of the blades in terms of both mean shape and roughness level, see Figure 22. The consequences of particle deposition range from performance degradation to life shortening to complete loss of power. Due to the importance of the phenomenon, models are being developed to predict the outcome of solid particle ingestion on gas turbine blades.

Suman et al [134] performed a very comprehensive analysis of the available data, using two non-dimensional parameters to describe the interaction between the incident particles and the substrate, with particular reference to sticking behaviour in a gas turbine. They examined historical experimental data on particle adhesion under gas turbine-like conditions through relevant dimensional quantities (e.g. particle viscosity, surface tension, and kinetic energy). The data were also divided into non-dimensional groups based on particle characteristics and identified impact conditions, with generic thresholds from erosion to deposition and from fragmentation to spattering. The relation between K (particle kinetic energy/surface energy) and Θ (the particle temperature normalized by the softening temperature) represents the basis of a promising adhesion criterion and predictive map of behaviour, see Figure 23.

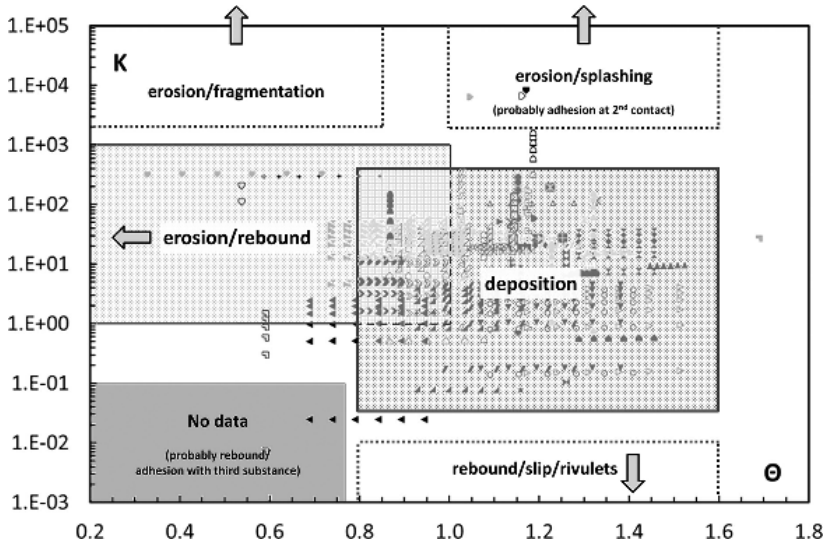

Figure 23 Impact behaviour map using non-dimensional groups K = E kin / E surf; _= T / T soft [134]

(a) (b)

Figure 24 Power generating steam turbine (a) Erosion of the blade (b) In-situ laser repaired blades (Reproduced from [135], with the permission of AIP Publishing)

Brandt and his co-workers reported that in-situ laser repairing (LC) using Stellite 6 onto steam turbine blades (AISI 420 martensitic stainless steel), which suffers from the similar damage as gas turbines, in a power station is feasible and practical using a fiber delivered diode laser and a robot, Figure 24 shows the leading edges of the turbine blades after LC. After one year, the turbine was inspected and the laser-repaired blades showed good performance without sign of damage [135, 136]. However, it should be noted that the repaired blades are thicker than the original blades, which suggests the form of the leading edge was changed.

5. Wind turbines

The renewable energy sources have seen a boom boosted by global efforts to combat climate change, such as the Paris Agreement, with wind energy leading the way.

Figure 25 shows the cumulative global wind power capacity installed over the past 19 years. By the end of 2019, the total global wind power capacity will be 651 gigawatts (GW), with a compound annual growth rate of about 12% over the past five years [137].

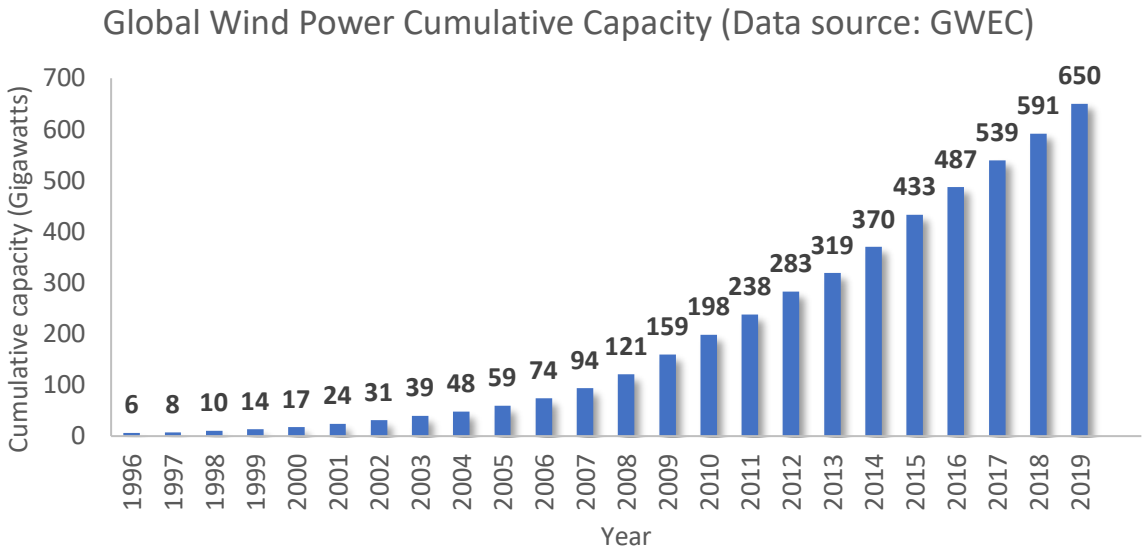

Figure 25 Historic development of total installations (onshore and offshore)

Wind turbines can be classified into horizontal axis wind turbines (HAWT) and vertical axis wind turbines (VAWT) according to the orientation of their main rotor axis. Measured by power coefficient, the current VAWT design lags behind the HAWT counterparts in terms of efficiency, and HAWT held

the major position in wind turbine designs. For lift-type wind turbine, the nomenclature of a typical blade design is shown in Figure 26. This type of turbine are very sensitive to changes in blade profile, design and surface roughness [138].

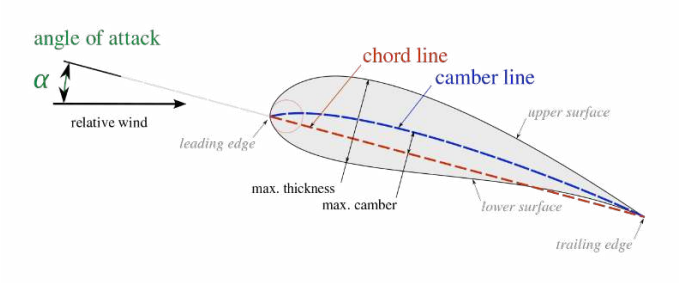

Figure 26 Blade aerofoil nomenclature [139]

High rotor efficiency is desired to increase wind energy extraction and maximize wind energy within the affordable production range. However, wind farms are plagued by poor performance compared to manufacturers' forecasts, and capacity factors are overestimated by 10 to 30 percent [140]. One of the main reasons is the change of roughness in blade leading edges, which leads to aerodynamic changes in the blade aerofoil, which has attracted much attention in numerical or experimental studies over the past decade [141-144].

The computational fluid dynamics (CFD) method is one of the most widely used wind turbine blade simulation methods to accurately predict the boundary layer and various unsteady flow characteristics resulting from blade leading edge roughness [145-148]. The experiments were conducted mainly using a pre-designed model of the damaged wing installed in a wind tunnel, where the leading edge damages were simulated based on the measurements of ex-serviced turbine blades [149, 150]. In particular, Pires conducted more practical tests in the field to further advance the understanding and modelling of blade surface roughness effects [151]. Both numerical and experimental studies have shown that surface roughness reduces the lift coefficient and increases the drag coefficient of the wing, especially at large angles of attack, leading to serious losses in wind power harvesting [16, 54, 152].

- Icing

Many of the frontier high-energy regions that wind farms seek to exploit, including northern Europe, have warm, humid and desert-like environments that typically provide conditions that are not conducive to turbine blade surfaces [144]. This section will look at those factors impact on wind turbine efficiency.

Wind turbines installed in cold climates can experience problems with ice build-up over their lifetime. Ice build-up on wind turbines, especially on turbine blades, can degrade turbine performance and durability. Continued ice accretion can significantly affect the structural loading of the entire rotor, leading to potentially hazardous conditions. Jasinski et al. identified that even the slight increase in surface roughness from onset of ice accretion could increases the drag coefficient and thereby reducing power production. Field data, wind tunnel simulations and numerical analyses have been employed to describe ice accretion on wind turbine blades. Aerodynamic coefficients and power curves were calculated to study the corresponding loads [153]. The annual energy production (AEP) loss for iced wind turbines is up to 17%, and the power factor reduction at harsh sites is typically in the range of 20 - 50% [154, 155].

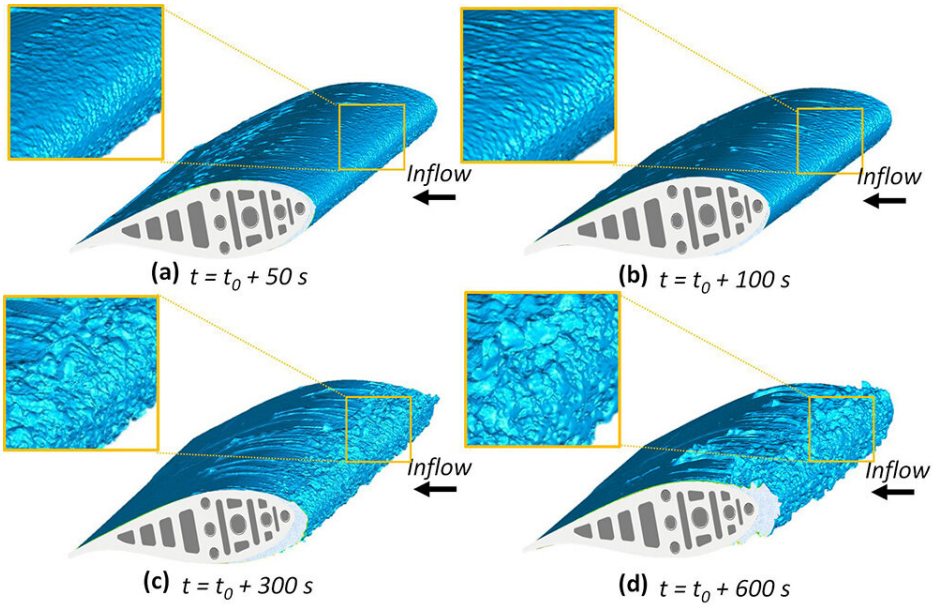

Figure 27 Time evolution of the 3D shapes of the ice structures accreted over the surface of the turbine blade model under a typical glaze icing condition of V_∞ = 40 m/s, LWC = 1.1 g/m3 and T_∞ = - 5.0 C [156]

An experimental study was performed in Icing Research Tunnel located at Iowa State University (ISU-IRT) with a typical glaze icing condition that wind turbines usually experience in cold and wet winters, V_∞ = 40 m/s, liquid water content (LWC) = 1.1 g/m^3 and $T_\infty = -5$℃. A Digital Image Projection (DIP) - based 3D scanning system was used to achieve 'in situ' measurements of the 3D shapes of the ice structures. Four representative instants, i.e., at 50 s, 100 s, 300 s and 600 s, after starting the ice accretion experiment were captured and shown in Figure 27 [156]. Characteristics of the dynamic ice accretion process on the turbine blade model were revealed clearly and quantitatively as a function of the ice accretion time. Quantitative measurements of 3D shape variations in ice structures accumulated on turbine blade models can be used to validate and verify various empirical and theoretical models used for ice accumulation prediction, and the findings from this study will also be very useful in improving our understanding of the potential icing physics associated with wind turbine icing phenomena, which is essential for the development of effective and robust de-icing/deicing strategies specifically targeting wind turbine icing mitigation measures.

- Insects

The power of wind turbines operating in high winds is reduced from 25 to 50 %, which is known as "double stall" or "multiple stall". Corten et al. attribute the occurrence of multiple stalls to the insect attachment, which states that these levels correspond to different levels of insect contamination. Low contamination levels can reduce power by up to 8% of the design value; at high levels, up to 55% can be reduced [41, 157]. Due to the mass inertia of the insect body, the insect can escape from the airflow streamlines and hit the blade if the air suddenly changes direction under the influence of an approaching rotor blade, see Figure 28 [158].

Corten proposed a hypothesis that the insect contamination was accumulated at low-wind speed, which thereby influence the turbine performance in high-wind running conditions. While the angle between the airflow and the blades increases under strong winds, the aerodynamic suction peak (minimum pressure and maximum wind speed of the area) has moved to the leading edge. If the leading edge is already covered with dead insects (from the low wind period onwards), the power output produced will drop. The greater the contamination at the suction peak, the faster the blade stall and the larger the loss of lift power. Therefore, the amount of insect contamination may change after each low wind period and result in different power levels being produced in high winds [41, 157]. The occurrence of stall

caused by leading edge roughness were validated by an experimental testing using stall flagging to compare airflow over smooth blades with that over blades whose leading edges were artificially roughened (by installing a zigzag tape of maximum thickness of 1.15 mm), see Figure 29.

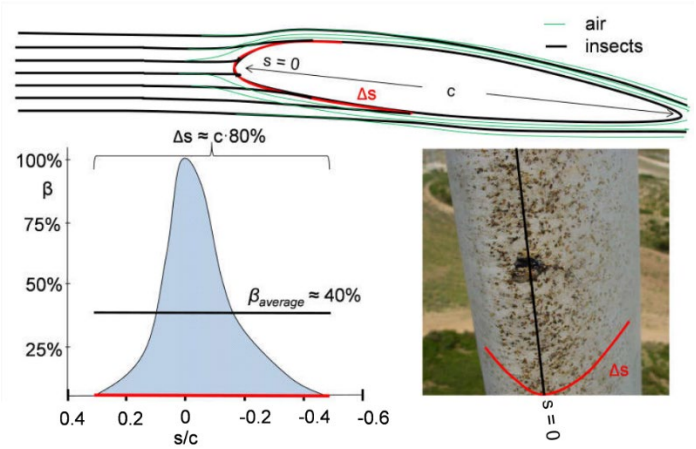

Figure 28 Approximation of the effective impact area of a rotor blade following the analysis of Wilcox & White (2016). Top: insect trajectories on an aerofoil (wrap distance s, leading edge at s=0, chord length c, impact length Δs (red line). Left: collection efficiency β as function of distance (s/c) from the leading edge (s=0) and the average integral collection efficiency βaverage assumed in the model. Variability depending on pitch angle and insect inertia is neglected. Right: Photo of insect residues (refer to Figure 3) explaining leading edge and impact length of a rotor blade as used in the model [158].

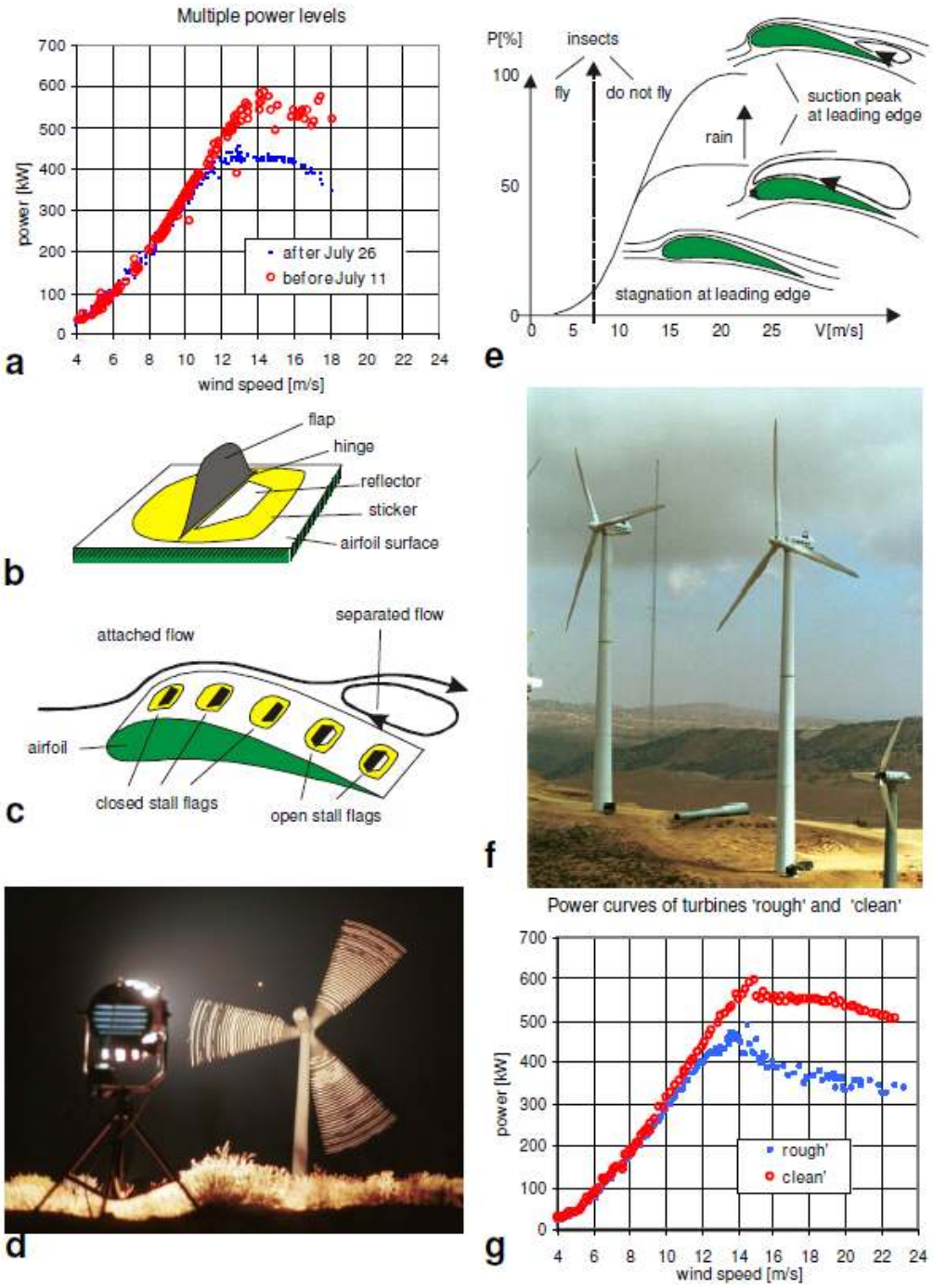

Figure 29 Insects cause multiple power levels from wind turbines. a, Example of two power levels at the same wind speed on different dates. b, The stall flag, consisting of a hinged flap and a reflector. c, Stall flags, showing the separated flow area on an aerofoil. d, Recording of stall flag signals from the NEG Micon turbine in California. The light tracks are produced by reflected light from open stall flags. e, Illustration of the insect hypothesis proposed to explain multiple power levels. f, The two turbines used for the validation of the insect hypothesis; these were only 50 m apart to ensure equal air inflow. g, The power curves for the two turbines with 'rough' and 'clean' blades, which are similar to those in a. [41]

- Erosion

Wind turbine blades are typically made of polymer-based composites, often bonded together. Many failure modes may develop from such a structure [159]. The HaliadeX-12 MW offshore wind turbine prototype in the Port of Rotterdam has set a new world record generating 288 MWh of continuous power in 24 hours and has a rotor size of 220 meters. The large diameter of the rotor allows the tip of

the wind turbine blades to reach a high linear speed range. In existing wind turbines, blade tip speeds of up to 100 m/s are reached [2], which thereby raise the leading edge erosion (LEE) of the blades as the turbine blade surface interacts with water droplets at high speeds [117].

The water droplet erosion (WDE) process on wind turbine blades typically begins with the formation of small pits near the leading edge, which increase in density over time and combine to form cracks and then grooves. Eventually, the cluster of grooves develops into a failure of material integrity, causing delamination near the leading edge [152, 160], see Figure 30.

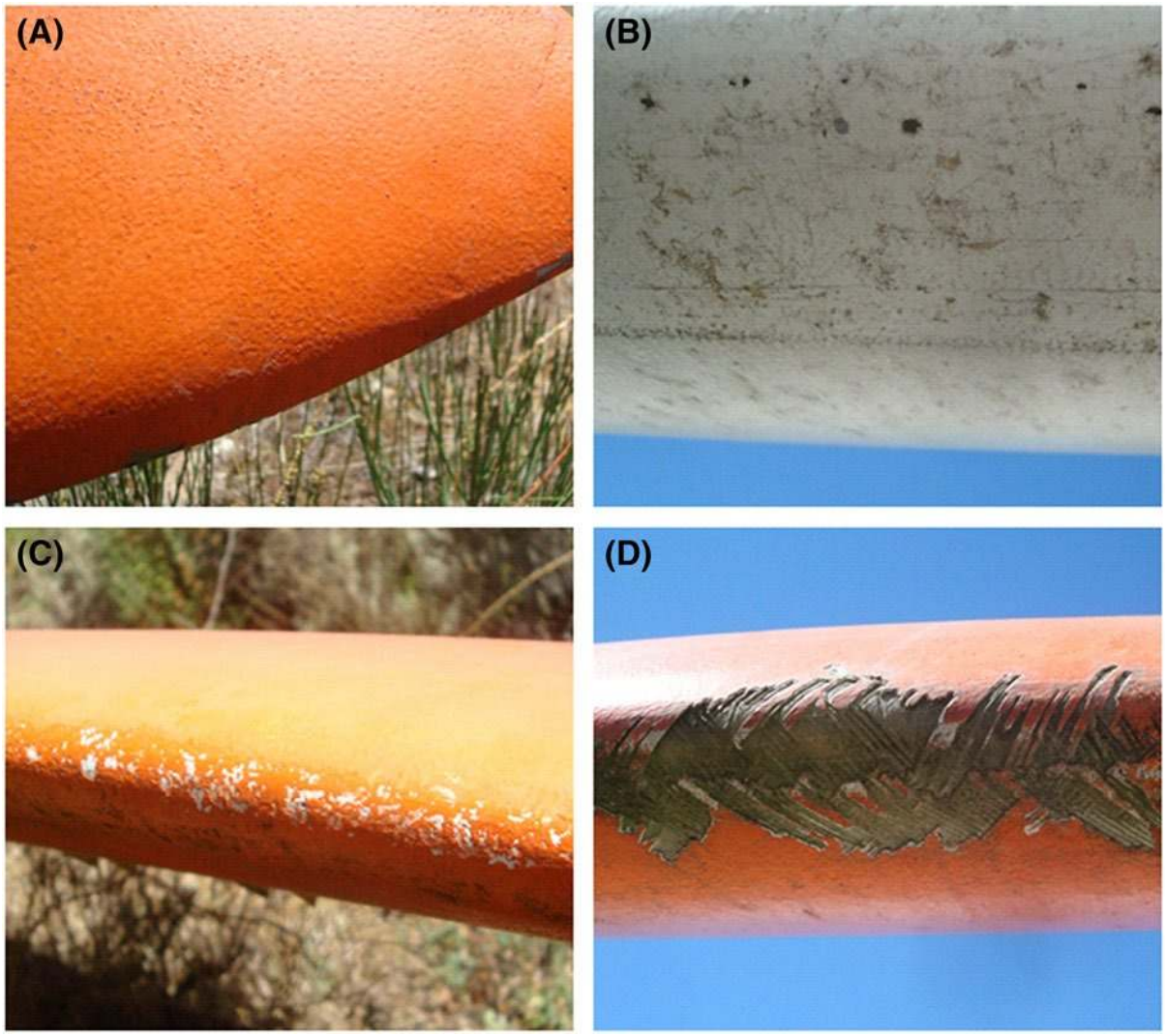

Figure 30 Progressive stages: A, pitting; B, cracking; C, cratering; and D, delamination, of the rain erosion on the leading edge of blades [160]

Erosions of the leading edge blades can significantly reduce blade performance, especially in the high speed rotor tip region, which is critical for optimizing blade performance and energy capture is critical. Studies have shown that for mild erosion, drag increases by about 6%, while for severe erosion, drag can increase by up to 500%. This equates to a 25% reduction in energy per year [152].

Effective protection methods that maintain leading edge form and roughness will provide significant benefits. As summarised by Herring, there are following options for protecting the leading edges of wind turbines; including coatings or tape system, erosion shields and integrated erosion shields. However, there appear to be several common failure themes, such as poor adhesion, which drives early separation, and poor manufacturing and application techniques, which introduce defects that lead to the

initiation of erosion [161]. Typically, operation and maintenance costs represent 20 - 25 % of the total cost per kilowatt-hour over the life of a wind turbine [162].

Apart from protective strategies, other techniques such as protuberance leading edges [163] and employing artificial intelligence to adaptive control the performance impact from leading edge roughness are being developed recently. An example was given in Figure 31, that operation and maintenance could be optimized based on the geometry of damaged blades. A comparison between adaptive and standard control is given in Table 2.

Table 2 Annual energy loss controlled though adaptive method [164]

Turbine	AEP (MWh)	AEP Loss (%)
Nominal	22,191	-
Damaged - adaptive control	20,213	8.9
Damaged - standard control	19,987	9.9

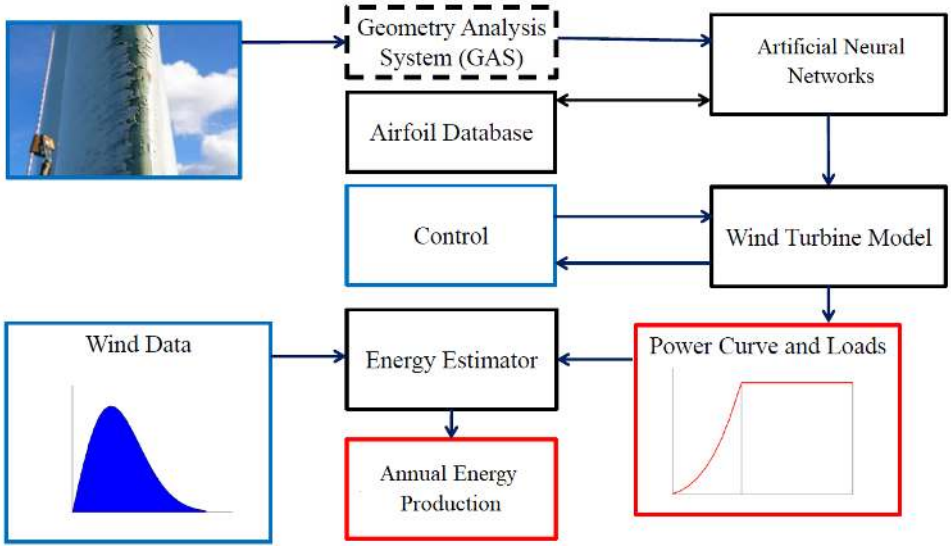

Figure 31 Adaptive control based on aerofoil force estimation of leading edge damaged blades [164].

6. Marine current turbines

The oceans provide an attractive renewable resource with the advantage of being predictable many days in advance, stable throughout the day and night, and the energy density is significantly higher compared to wind and solar energy [165-169]. As a result, efforts have been made over the past 20 years to develop tidal turbines, which have now reached the stage of commercialization [170]. However, the performance of the turbine can be significantly reduced by the increasing roughness on the marine current turbine blades [171]. The two main potential performance issues for marine current turbines identified by Fraenkel [172] and Ng et al. [173], including the roughening of the turbine blades due to impact, cavitation or scour due to particulates; and the fouling of the turbine blades by marine growth. They also point out the need for high reliability in view of the difficulty of maintenance in the underwater environment.

The biggest threat is fouling caused by marine organisms, which has a profound impact on the levelized cost of energy (LCOE) due to its impact on the maintenance schedule of turbine blades [170]. Figure 32 present photos taken just after 6 months after the turbine has been deployed into the sea (Clean Current Tidal Power Demonstration Project), and the scratches on the blades show the thickness of the diatoms [174]. Fouling on tidal turbine blades develops at an alarming rate, whereas tidal energy systems are designed to operate for 20-25 years [170].

(a) (b)

Figure 32 (a) Fouling after 6 month (b) Encrustations of diatoms or hydroids on blade (Clean Current Tidal Power Demonstration Project) [170, 174]

Orme et al. investigated the effect of barnacles on the lift and drag coefficients of airfoils covered with idealized and uniformly distributed barnacles. By comparing the results of the experiments conducted in the wind tunnel, it was concluded that as the barnacle size and distribution density increase, the lift-to-resistance ratio decreases and their presence will adversely affect the efficiency of the turbine [175]. Song numerically studied the effect of roughness or fouling on the sea current turbine by CFD method, and the significant decrease of power coefficient and the change of optimal operating conditions caused by roughness were also observed [176]. Walker's study have shown that the presence of roughness or fouling increases the drag coefficient by 75% and that the lift behaviour in unsteady flow may be very different from that in steady flow [177]. It should be noted that Walker's study was conducted with the barnacle attached to the upper (suction) surface, whereas Song's model simulated the distribution of barnacles over the entire leaf surface (including the leading edge).

7. Marine propellers

The increase in energy consumption of marine systems indicates one or more of the main components that related to the marine efficiency are being adversely effected. These are the ship's hydrodynamic system, namely hull drag, propulsion efficiency and hull-propeller interaction. Such aspects can be resolved in many ways, both in terms of design and operation. Marine propellers operate in a harsh environment, that they can be damaged by impact from floating debris and underwater objects. They may also subject to corrosion and cavitation erosion [178]. They will suffer erosion corrosion in use and biofouling particularly when docked.

From the operational perspective, marine biofouling is a growing problem and even a small amount of biofouling can lead to a significant increase in fuel consumption. It is vital to mitigate its impact on ship's hull because of its adverse effects on ship efficiency, increased GHG emissions and transportation of harmful non-indigenous species. It is equally important to investigate the level of biofouling on the propeller, and understand their potential impact [179] and accurately model the accumulation of fouling and retrofit it with new antifouling coating. With the increase in computing power, the use of numerical programs is becoming increasingly popular to help diagnose the biofouling problem on marine propeller [180]. Other than biofouling, as the marine propeller operates under high rotational speed and under heavy load that transfer rotational motion into thrust, the huge drop of pressure between the upstream and downstream of propeller surface leads to vulnerability to cavitation damage. The propellers are therefore subject to corrosion, and cavitation erosion [181, 182]. They are may also subject to impact damage from floating debris and submerged objects.

As studied by [183], the pressure on the upstream surface of the blade can drop below the vapor pressure result in the formation of a vapor pocket. The cavitation bubbles form at the area of low pressure, and then flow to propeller of high pressure, causing the vapor pocket explosion; the collapse of cavitation bubbles creates shock waves and hence cavitation noise that also influence the comfort of cruising ship.

The cavitation initially occurs in the region of boundary layer. The cavitation results in different size of pits on blade leading edge which accelerate the erosion and fouling phenomenon and also, the roughened surfaces transfers the boundary layer from laminar to turbulent flow that further reduce the performance and efficiency of the marine propeller [184].

A recent study [185] performed experimental studies to investigate foul release coatings and their cavitation resistance and antifouling properties on marine propeller. Sponges and other soft fouling were found to be easily removed after cleaning, the non-toxic fouling release propeller coating was also resistant against hard dirt. These are necessary to maintain high propulsion efficiency and prolong the life of the propeller.

8. Conclusions

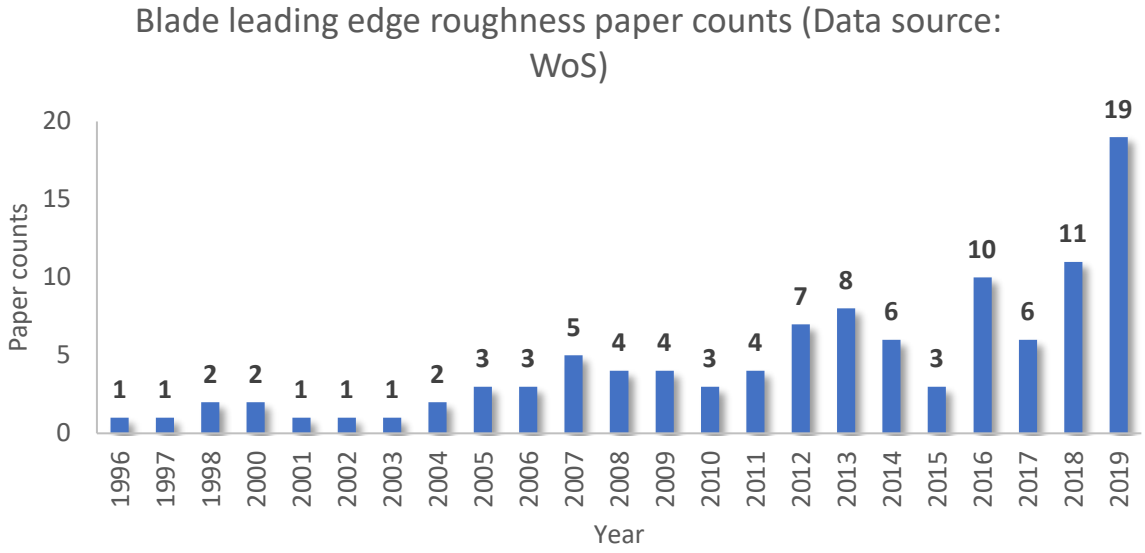

Figure 33 Paper count over the past 20 years for key words: blade leading edge roughness (source from web of science)

There is a growing library of research papers dedicated to roughness and form effects of blade leading edges in turbomachinery, see Figure 33. This review found over 180 papers mainly in the past 20 years. With the majority looking at leading edges of blades from the various stages of aeroengine and gas turbines. There is growing awareness of the importance of controlling roughness and the form of leading edge on other turbomachinery designs such as wind and marine tidal turbines and rotorcraft. However, it has been difficult to be critically review this subject as, until recently, blade leading edges have not had much attention in relationship to their importance in the performance of turbomachines and the subsequent economic and environmental impact they have. Only recently have their importance come into focus through engine test results and modelling. These show a drop in efficiency that increased fuel burn by 1% on commercial aircraft and up to 50% drop in efficiency for wind turbine blades covered with insects. Both additive and subtractive roughness processes on blade leading edges can cause significant drops in turbomachinery performance. From an efficiency point of view, additive processes are typically worse than subtractive processes, as the roughness or even form change is significant with icing and biofouling. Table 3 summarises the dominant mechanisms of roughness variation for individual applications discussed in this paper, with different colors indicating the corresponding severity of the mechanisms for these applications. There are gaps in the current understanding of the additive and subtractive processes that influence roughness and their interaction. Antagonism is reported between additive and subtractive roughness processes and these can result in smoother surfaces (i.e. insect deposition and water droplet impingement).

Table 3 Summary of dominant roughness change mechanisms according to applications (Red: serious, Orange: medium, Gold: light)

	Insect	Icing	Marine biofouling	Particle attachment	Solid particle erosion	Water droplet erosion	Cavitation /corrosion	Foreign object damage
Turbofan	Intake fan	Intake fan Compressor		Compressor Turbine	Intake fan Compressor Turbine	Intake fan		Intake fan Compressor turbine
Gas turbines				Compressor Turbine	Intake fan Compressor Turbine	Compressor		Intake fan Compressor Turbine
Wind turbine								
Tidal turbine								
Ship propeller								

The literature shows a need for more data from in-service and laboratory rigs as well as predictive models for additive and subtractive roughness and change in form processes and the synergy/antagonism between mechanisms. The range changes of roughness / form seen cover nm to cm level. Measuring the roughness of soft biofouling is a particular challenge and requires non-contact techniques [186]. Also as recent work on fan blades showed, there is still a lack of complete understanding of the subtractive mechanisms or the physics behind them or their interaction with the microstructure/ material. Therefore, it is not clear what mechanism should be modelled to allow a prediction of roughness evolution and therefore performance or optimal operating conditions. There also needs to be better monitoring of the service conditions and their consequences on the leading edges and thus performance.

Recent work paves the way where and for machine learning to be used to predict coated wind turbine blade leading edge delamination and the effects this has on aerodynamic performance and what changes in blade angle etc would best capture the available wind energy with damaged blades [164]. To do this more generically, there is a need to better understanding the environment the blades operates within. There is also a need understand the variation of conditions along their length along with the blade material or coated material response to additive and/or subtractive mechanisms and thus the roughness/form evolution over time. This is turn would allow better understanding of the effects these changes have on aerodynamic/ hydrodynamic efficiency and the population of stress raisers and distribution of residual stresses that result which influence fatigue strength and remaining useful life as well as inform maintenance/repair needs. The recent, map and root cause analysis of various damage mechanisms in gas turbines is a good start [98], so if rebound or deposition or splash or erosion from particle impacts can be predicted but the resulting topography needs to be generated so research should focus on delivering this and feeding into flow models to predict efficiency / performance data.

To prevent degradation to leading edges there is a need to understand the physics of erosion on surface engineered edges and coated surfaces to control roughness and extend the incubation period and thereby maintain efficiency and extend service life. The ideal coating needs to control roughness and impede material loss to retain the leading edge profile. For blades that have been reprofiled, blended, coated, surface treated, weld overlayed or laser cladded then their leading edge roughness will be determined by these processes and may well differ from the original edge roughness. Hence, repaired blades will behave differently aerodynamically as well as have different mechanical properties that will affect damage tolerance and fatigue strength.

References:

[1] H. Slot, E. Gelinck, C. Rentrop, and E. Van Der Heide, "Leading edge erosion of coated wind turbine blades: Review of coating life models," *Renewable Energy,* vol. 80, pp. 837-848, 2015.

[2] M. H. Keegan, D. Nash, and M. Stack, "On erosion issues associated with the leading edge of wind turbine blades," *Journal of Physics D: Applied Physics,* vol. 46, no. 38, p. 383001, 2013.

[3] Delta TechOps (DTO), MDS Coating Technologies (MCT), and America's Phenix Inc. (AP), "Leading edge protective coating against fluid and particulate erosion for turbofan blades," *Presented to FAA Office of Environment and Energy,* 2018.

[4] D. Alman and D. Marcio, "Erosion-Resistant Nanocoatings for Improved Energy Efficiency in Gas Turbines," National Energy Technology Lab.(NETL), Pittsburgh, PA, and Morgantown, WV …, 2014.

[5] G. F. Schmitt Jr, "Coatings for erosion resistance," in *Proceedings of 37th Meeting–Mechanical Properties, Performance and Failure Modes of Coatings, Cambridge University Press*, 1984, pp. 148-164.

[6] C. J. Bai, W. C. Wang, and P. W. Chen, "The effects of sinusoidal leading edge of turbine blades on the power coefficient of horizontal-axis wind turbine (HAWT)," *International journal of green energy,* vol. 13, no. 12, pp. 1193-1200, 2016.

[7] O. Stalnov, A. Kribus, and A. Seifert, "Evaluation of active flow control applied to wind turbine blade section," *Journal of Renewable and Sustainable Energy,* vol. 2, no. 6, p. 063101, 2010.

[8] C. J. Bai, Y. Y. Lin, S. Y. Lin, and W. C. Wang, "Computational fluid dynamics analysis of the vertical axis wind turbine blade with tubercle leading edge," *Journal of Renewable and Sustainable Energy,* vol. 7, no. 3, p. 033124, 2015.

[9] S. Aftab, N. Razak, A. M. Rafie, and K. Ahmad, "Mimicking the humpback whale: An aerodynamic perspective," *Progress in Aerospace Sciences,* vol. 84, pp. 48-69, 2016.

[10] M. D. Bolzon, R. M. Kelso, and M. Arjomandi, "Tubercles and their applications," *Journal of aerospace engineering,* vol. 29, no. 1, p. 04015013, 2016.

[11] R. Pérez-Torró and J. W. Kim, "A large-eddy simulation on a deep-stalled aerofoil with a wavy leading edge," *Journal of Fluid Mechanics,* vol. 813, pp. 23-52, 2017.

[12] F. E. Fish, P. W. Weber, M. M. Murray, and L. E. Howle, "Marine applications of the biomimetic humpback whale flipper," *Marine Technology Society Journal,* vol. 45, no. 4, pp. 198-207, 2011.

[13] F. E. Fish and J. M. Battle, "Hydrodynamic design of the humpback whale flipper," *Journal of Morphology,* vol. 225, no. 1, pp. 51-60, 1995.

[14] F. Fish and G. V. Lauder, "Passive and active flow control by swimming fishes and mammals," *Annu. Rev. Fluid Mech.,* vol. 38, pp. 193-224, 2006.

[15] D. Miklosovic, M. Murray, L. Howle, and F. Fish, "Leading-edge tubercles delay stall on humpback whale (Megaptera novaeangliae) flippers," *Physics of fluids,* vol. 16, no. 5, pp. L39-L42, 2004.

[16] Y. Zhang, M. Zhang, and C. Cai, "Flow control on wind turbine airfoil affected by the surface roughness using leading-edge protuberance," *Journal of Renewable and Sustainable Energy,* vol. 11, no. 6, p. 063304, 2019.

[17] J. A. Sładek, *Coordinate Metrology*. Springer, 2016.

[18] B. Chao, H. Liu, L. Bao, and D. Li, "Study on measurement of leading and trailing edges of blades based on optical scanning system," in *AOPC 2017: 3D Measurement Technology for Intelligent Manufacturing*, 2017, vol. 10458: International Society for Optics and Photonics, p. 104580R.

[19] G. Budzik *et al.*, "Analysis of dimensional accuracy of blade of aircraft engine using a coordinate measuring machine," *Journal of KONES,* vol. 21, 2014.

[20] Y. Li and P. Gu, "Free-form surface inspection techniques state of the art review," *Computer-Aided Design,* vol. 36, no. 13, pp. 1395-1417, 2004.

[21] M. Magdziak, "An algorithm of form deviation calculation in coordinate measurements of free-form surfaces of products," *Strojniški vestnik-Journal of Mechanical Engineering,* vol. 62, no. 1, pp. 51-59, 2016.

[22] W. Jakubiec, M. Wojtyła, and W. Płowucha, "Research on accuracy of the V-probe in measurement of bended pipe elements," in *Proc. of the 1st Inter. Conference "Quality and Innovation in Engineering and Management". Cluj-Napoca*, 2011, pp. 105-108.

[23] X. Zhicong, H. Zhong, B. Yulei, B. Hong, S. Zuochun, and Z. Yanzhou, "High-precision measurement for the three-dimensional profile of gas turbine blade's leading edge," *Journal of Aerospace Power, Papers,* vol. 31, no. 7, pp. 1761-1765, 2016.

[24] A. Kawalec and M. Magdziak, "The selection of radius correction method in the case of coordinate measurements applicable for turbine blades," *Precision Engineering,* vol. 49, pp. 243-252, 2017.

[25] A. Shihavuddin *et al.*, "Wind turbine maintenance cost reduction by deep learning aided drone inspection analysis," 2019.

[26] E. K. Kruse, "A Method for Quantifying Wind Turbine Leading Edge Roughness and its Influence on Energy Production," DTU Wind Energy, 2019.

[27] R. Kurz and K. Brun, "Fouling mechanisms in axial compressors," *Journal of engineering for gas turbines and power,* vol. 134, no. 3, 2012.

[28] A. Hansen and C. Butterfield, "Aerodynamics of horizontal-axis wind turbines," *Annual Review of Fluid Mechanics,* vol. 25, no. 1, pp. 115-149, 1993.

[29] W. Batten, A. Bahaj, A. Molland, and J. Chaplin, "The prediction of the hydrodynamic performance of marine current turbines," *Renewable energy,* vol. 33, no. 5, pp. 1085-1096, 2008.

[30] Y. Boluk, "Adhesion of freezing precipitates to aircraft surfaces," 1996.

[31] S. M. Fikke *et al.*, *COST 727: atmospheric icing on structures: measurements and data collection on icing: state of the art*. Meteo Schweiz, 2006.

[32] F. Richert, "Is Rotorcraft icing knowledge transferable to wind turbines," *BOREAS III. FMI, Saariselkä, Finland,* pp. 366-380, 1996.

[33] O. Parent and A. Ilinca, "Anti-icing and de-icing techniques for wind turbines: Critical review," *Cold regions science and technology,* vol. 65, no. 1, pp. 88-96, 2011.

[34] O. Fakorede, Z. Feger, H. Ibrahim, A. Ilinca, J. Perron, and C. Masson, "Ice protection systems for wind turbines in cold climate: characteristics, comparisons and analysis," *Renewable and Sustainable Energy Reviews,* vol. 65, pp. 662-675, 2016.

[35] S. T. McClain, M. Vargas, J.-C. Tsao, A. P. Broeren, and S. Lee, "Ice accretion roughness measurements and modeling," 2017.

[36] A. Hardy and P. Milne, "Studies in the distribution of insects by aerial currents," *The Journal of Animal Ecology,* pp. 199-229, 1938.

[37] S. Vogel, "Flight in Drosophila: III. Aerodynamic characteristics of fly wing sand wing models," *Journal of Experimental Biology,* vol. 46, no. 3, pp. 431-443, 1967.

[38] W. Nachtigall, *Insects in flight*. HarperCollins Publishers LLC, New York., 1974.

[39] C. C. Voigt, "Insect fatalities at wind turbines as biodiversity sinks," *Conservation Science and Practice,* p. e366, 2021.

[40] G. Fiore and M. S. Selig, "A simulation of operational damage for wind turbine blades," in *32nd AIAA Applied Aerodynamics Conference*, 2014, p. 2848.

[41] G. P. Corten and H. F. Veldkamp, "Insects can halve wind-turbine power," *Nature,* vol. 412, no. 6842, pp. 41-42, 2001.

[42] R. S. Ehrmann, B. Wilcox, E. B. White, and D. C. Maniaci, "Effect of Surface Roughness on Wind Turbine Performance," Sandia National Lab.(SNL-NM), Albuquerque, NM (United States), 2017.

[43] W. Han, J. Kim, and B. Kim, "Effects of contamination and erosion at the leading edge of blade tip airfoils on the annual energy production of wind turbines," *Renewable energy,* vol. 115, pp. 817-823, 2018.
[44] C. Spruce, "Power performance of active stall wind turbines with blade contamination," in *Proceedings of the European Wind Energy Conference*, 2006.
[45] W. S. Coleman, "The characteristics of roughness from insects as observed for two-dimensional, incompressible flow past airfoils," *Journal of the Aerospace Sciences,* vol. 26, no. 5, pp. 264-280, 1959.
[46] E. Moroz and D. Eggleston, "A comparison between actual insect contamination and its simulation," in *Wind Power*, 1992, vol. 7, pp. 418-425.
[47] C. C. Croom and B. J. Holmes, "Insect contamination protection for laminar flow surfaces," 1986.
[48] M. Kok, D. Raps, and T. M. Young, "Effects of surface roughness and energy on insect residue adhesion to aircraft leading edge surfaces," in *Proceeding of the 36th annual meeting of the adhesion society, Daytona Beach, USA*, 2013, pp. 3-6.
[49] C. C. Stringer and B. L. Polagye, "Implications of biofouling on cross-flow turbine performance," *SN Applied Sciences,* vol. 2, no. 3, pp. 1-13, 2020.
[50] M. E. Callow and J. A. Callow, "Marine biofouling: a sticky problem," *Biologist,* vol. 49, no. 1, pp. 1-5, 2002.
[51] P. Shivapooja, "Active Surface Deformation Technology for Management of Marine Biofouling," Doctoral dissertation, Duke University, 2016.
[52] M. Pérez, M. Stupak, G. Blustein, M. Garcia, and L. M. Lindblad, "Organic alternatives to copper in the control of marine biofouling," in *Advances in Marine Antifouling Coatings and Technologies*: Elsevier, 2009, pp. 554-571.
[53] A. G. Nurioglu and A. C. C. Esteves, "Non-toxic, non-biocide-release antifouling coatings based on molecular structure design for marine applications," *Journal of Materials Chemistry B,* vol. 3, no. 32, pp. 6547-6570, 2015.
[54] E. Sagol, M. Reggio, and A. Ilinca, "Issues concerning roughness on wind turbine blades," *Renewable and Sustainable Energy Reviews,* vol. 23, pp. 514-525, 2013.
[55] M. F. Kerho and M. B. Bragg, "Airfoil boundary-layer development and transition with large leading-edge roughness," *AIAA journal,* vol. 35, no. 1, pp. 75-84, 1997.
[56] M. P. Schultz and G. W. Swain, "The influence of biofilms on skin friction drag," *Biofouling,* vol. 15, no. 1-3, pp. 129-139, 2000.
[57] H. Barnes and H. T. Powell, "The development, general morphology and subsequent elimination of barnacle populations, Balanus crenatus and B. balanoides, after a heavy initial settlement," *The Journal of Animal Ecology,* pp. 175-179, 1950.
[58] N. Casari, M. Pinelli, A. Suman, L. Di Mare, and F. Montomoli, "Gas turbine blade geometry variation due to fouling," in *12th European Conference on Turbomachinery Fluid Dynamics and Thermodynamics, ETC 2017*, 2017: KTH Royal Institute of Technology, pp. 1-10.
[59] R. J. Clarkson, E. J. Majewicz, and P. Mack, "A re-evaluation of the 2010 quantitative understanding of the effects volcanic ash has on gas turbine engines," *Proceedings of the Institution of Mechanical Engineers, Part G: Journal of Aerospace Engineering,* vol. 230, no. 12, pp. 2274-2291, 2016.
[60] A. Hamed, W. Tabakoff, and R. Wenglarz, "Erosion and deposition in turbomachinery," *Journal of propulsion and power,* vol. 22, no. 2, pp. 350-360, 2006.
[61] P. L. Menezes, M. Nosonovsky, S. P. Ingole, S. V. Kailas, and M. R. Lovell, *Tribology for scientists and engineers*. Springer, 2013.
[62] M. Shinozaki, K. A. Roberts, B. van de Goor, and T. W. Clyne, "Deposition of ingested volcanic ash on surfaces in the turbine of a small jet engine," *Advanced Engineering Materials,* vol. 15, no. 10, pp. 986-994, 2013.

[63] O. Gohardani, "Impact of erosion testing aspects on current and future flight conditions," *Progress in Aerospace Sciences,* vol. 47, no. 4, pp. 280-303, 2011.
[64] A. Standard, "G73, 2010, Standard test method for liquid impingement erosion using rotating apparatus," ed: ASTM International, West Conshohocken, PA, 2010.
[65] C. B. Burson-Thomas, R. Wellman, T. J. Harvey, and R. J. Wood, "Importance of Surface Curvature in Modeling Droplet Impingement on Fan Blades," *Journal of Engineering for Gas Turbines and Power,* vol. 141, no. 3, 2019.
[66] D. Ma, "Rain erosion protection for fan blades," University of Southampton, 2018.
[67] A. Sayma, M. Kim, and N. Smith, "Leading-edge shape and aeroengine fan blade performance," *Journal of propulsion and power,* vol. 19, no. 3, pp. 517-520, 2003.
[68] H. Kirols, D. Kevorkov, A. Uihlein, and M. Medraj, "Water droplet erosion of stainless steel steam turbine blades," *Materials Research Express,* vol. 4, no. 8, p. 086510, 2017.
[69] H. Law and V. Koutsos, "Leading edge erosion of wind turbines: Effect of solid airborne particles and rain on operational wind farms," *Wind Energy,* vol. 23, no. 10, pp. 1955-1965, 2020.
[70] F. G. Hammitt, "Damage to solids caused by cavitation," *Philosophical Transactions for the Royal Society of London. Series A, Mathematical and Physical Sciences,* pp. 245-255, 1966.
[71] T. Keil, P. Pelz, J. Kadavelil, J. Necker, W. Moser, and D. Christ, "Droplet impact vs. cavitation erosion," in *Proceedings of WIMRC 3rd International Cavitation Forum, 4th-6th July*, 2011, p. 2011.
[72] C. M. Preece and J. H. Brunton, "A comparison of liquid impact erosion and cavitation erosion," *Wear,* vol. 60, no. 2, pp. 269-284, 1980.
[73] P. Wu, L. Bai, W. Lin, and X. Wang, "Mechanism and dynamics of hydrodynamic-acoustic cavitation (HAC)," *Ultrasonics sonochemistry,* vol. 49, pp. 89-96, 2018.
[74] G. Yang *et al.*, *Handbook of ultrasonics and sonochemistry*. Springer, 2016.
[75] J. Liang, Y. An, and W. Chen, "Tb (III) line intensities in multibubble sonoluminescence," *Ultrasonics sonochemistry,* vol. 58, p. 104688, 2019.
[76] H. Xu, N. G. Glumac, and K. S. Suslick, "Temperature inhomogeneity during multibubble sonoluminescence," *Angewandte Chemie,* vol. 122, no. 6, pp. 1097-1100, 2010.
[77] R. Pflieger, S. I. Nikitenko, and M. Ashokkumar, "Effect of NaCl salt on sonochemistry and sonoluminescence in aqueous solutions," *Ultrasonics sonochemistry,* vol. 59, p. 104753, 2019.
[78] O. Supponen, D. Obreschkow, P. Kobel, M. Tinguely, N. Dorsaz, and M. Farhat, "Shock waves from nonspherical cavitation bubbles," *Physical Review Fluids,* vol. 2, no. 9, p. 093601, 2017.
[79] X. Ma *et al.*, "Comparisons of spark-charge bubble dynamics near the elastic and rigid boundaries," *Ultrasonics sonochemistry,* vol. 43, pp. 80-90, 2018.
[80] X. Wu, J. Liu, and J.-J. Zhu, "Sono-Fenton hybrid process on the inactivation of Microcystis aeruginosa: Extracellular and intracellular oxidation," *Ultrasonics sonochemistry,* vol. 53, pp. 68-76, 2019.
[81] P. Wu, L. Bai, and W. Lin, "On the definition of cavitation intensity," *Ultrasonics Sonochemistry,* vol. 67, p. 105141, 2020/10/01/ 2020, doi: https://doi.org/10.1016/j.ultsonch.2020.105141.
[82] M. O'Donnell, "Foreign Object Debris/Damage (FOD) Detection Equipment," *Advisory circular of US department of transportation, Federal Aviation Administration,* vol. 10, 2009.
[83] H. Xu, Z. Han, S. Feng, H. Zhou, and Y. Fang, "Foreign object debris material recognition based on convolutional neural networks," *Eurasip Journal on Image and Video Processing,* vol. 2018, no. 1, p. 21, 2018.
[84] "FOD Prevention Manual," *CAAC Airport Division, et al.,* 2009.
[85] X. Chen and J. W. Hutchinson, "Particle impact on metal substrates with application to foreign object damage to aircraft engines," *Journal of the Mechanics and Physics of Solids,* vol. 50, no. 12, pp. 2669-2690, 2002.
[86] T. Nicholas, J. Barber, and R. S. Bertke, "Impact damage on titanium leading edges from small hard objects," *Experimental Mechanics,* vol. 20, no. 10, pp. 357-364, 1980.

[87] S. Hudak, K. Chan, R. McClung, G. Chell, Y. Lee, and D. Davidson, "High cycle fatigue of turbine blade materials," Final technical report UDRI subcontract no. RI 40098X SwRI project, 1999.
[88] J. Peters, B. Boyce, A. Thompson, R. Ritchie, and O. Roder, "Role of foreign-object damage on thresholds for high-cycle fatigue in Ti-6Al-4V," *Metallurgical and Materials Transactions A,* vol. 31, no. 6, pp. 1571-1583, 2000.
[89] S. Spanrad and J. Tong, "Characterisation of foreign object damage (FOD) and early fatigue crack growth in laser shock peened Ti–6Al–4V aerofoil specimens," *Materials Science and Engineering: A,* vol. 528, no. 4-5, pp. 2128-2136, 2011.
[90] A. R. Kristnama, X. Xu, D. Nowell, M. R. Wisnom, and S. R. Hallett, "Experimental investigation of high velocity oblique impact and residual tensile strength of carbon/epoxy laminates," *Composites Science and Technology,* vol. 182, p. 107772, 2019.
[91] Y. Xu, L. Cheng, C. Shu, X. Chen, and P. Li, "Foreign Object Damage Performance and Constitutive Modeling of Titanium Alloy Blade," *International Journal of Aerospace Engineering,* vol. 2020, 2020.
[92] C. Shakal. "Trent 900 Turbofan, https://grabcad.com/library/trent-900-turbofan-1." (accessed 2021).
[93] E. National Academies of Sciences and Medicine, *Commercial aircraft propulsion and energy systems research: reducing global carbon emissions*. National Academies Press, 2016.
[94] S. Kumari, D. Satyanarayana, and M. Srinivas, "Failure analysis of gas turbine rotor blades," *Engineering failure analysis,* vol. 45, pp. 234-244, 2014.
[95] R. Dewangan, J. Patel, J. Dubey, P. K. Sen, and S. K. Bohidar, "Gas turbines blades-a critical review of failure on first and second stages," *Int J Mech Eng Robot Res,* vol. 4, no. 1, pp. 216-223, 2015.
[96] V. N. B. Rao, I. N. Kumar, K. B. Prasad, N. Madhulata, and N. Gurajarapu, "Failure mechanisms in turbine blades of a gas turbine Engine–an overview," *Int. J. Eng. Res. Dev,* vol. 10, pp. 48-57, 2014.
[97] S. Rani, "Common failures in gas turbine blade: A critical review," *Int. J. Eng. Sci. Res. Technol,* vol. 3, pp. 799-803, 2018.
[98] J. Aust and D. Pons, "Taxonomy of Gas Turbine Blade Defects," *Aerospace,* vol. 6, no. 5, p. 58, 2019.
[99] E. Syverud, "Axial compressor performance deterioration and recovery through online washing," 2007.
[100] A. A. Hamed, W. Tabakoff, R. B. Rivir, K. Das, and P. Arora, "Turbine blade surface deterioration by erosion," 2005.
[101] M. G. Dunn, C. Padova, J. Moller, and R. Adams, "Performance deterioration of a turbofan and a turbojet engine upon exposure to a dust environment," 1987.
[102] H. De Ryck, "Turbofan design for the commercial aircraft," ed: Warsaw University of Technology, Warsaw, Poland, 2008.
[103] A. Ghenaiet, "Study of sand particle trajectories and erosion into the first compression stage of a turbofan," *Journal of turbomachinery,* vol. 134, no. 5, 2012.
[104] D. Ma, T. J. Harvey, R. G. Wellman, and R. J. Wood, "Characterisation of rain erosion at ex-service turbofan blade leading edges," *Wear,* vol. 426, pp. 539-551, 2019.
[105] A. Gujba, L. Hackel, D. Kevorkov, and M. Medraj, "Water droplet erosion behaviour of Ti–6Al–4V and mechanisms of material damage at the early and advanced stages," *Wear,* vol. 358, pp. 109-122, 2016.
[106] M. Willshee, "Compressor deterioration," 1999/2000.
[107] M. N. Goodhand and R. J. Miller, "Compressor leading edge spikes: a new performance criterion," *Journal of turbomachinery,* vol. 133, no. 2, 2011.
[108] K. Walton, L. Blunt, L. Fleming, M. Goodhand, and H. Lung, "Areal parametric characterisation of ex-service compressor blade leading edges," *Wear,* vol. 321, pp. 79-86, 2014.

[109] P. Gilge, A. Kellersmann, J. Friedrichs, and J. R. Seume, "Surface roughness of real operationally used compressor blade and blisk," *Proceedings of the Institution of Mechanical Engineers, Part G: Journal of Aerospace Engineering,* vol. 233, no. 14, pp. 5321-5330, 2019.
[110] J.-P. Stalder, "Gas turbine compressor washing state of the art: Field experiences," *J. Eng. Gas Turbines Power,* vol. 123, no. 2, pp. 363-370, 2001.
[111] M. Bojdo and A. Filippone, "Effect of desert particulate composition on helicopter engine degradration rate," 2014.
[112] P. Patnaik, M. Pishva, J. Elder, W. Doswell, and R. Thamburaj, "Repair and life extension of titanium alloy fan blades in aircraft gas turbines," in *Turbo Expo: Power for Land, Sea, and Air*, 1989, vol. 79177: Citeseer, p. V005T11A004.
[113] E. Kablov and S. Muboyadzhyan, "Erosion-resistant coatings for gas turbine engine compressor blades," *Russian Metallurgy (Metally),* vol. 2017, no. 6, pp. 494-504, 2017.
[114] R. Wellman and J. Nicholls, "A review of the erosion of thermal barrier coatings," *Journal of Physics D: Applied Physics,* vol. 40, no. 16, p. R293, 2007.
[115] A. P. Charles and C. A. Gonzalez Taylor, "Development of a method to repair gas turbine blades using electron beam melting additive manufacturing technology," ed, 2017.
[116] X. Yang *et al.*, "Removal and repair techniques for thermal barrier coatings: a review," *Transactions of the IMF,* vol. 98, no. 3, pp. 121-128, 2020.
[117] M. Elhadi Ibrahim and M. Medraj, "Water Droplet Erosion of Wind Turbine Blades: Mechanics, Testing, Modeling and Future Perspectives," *Materials,* vol. 13, no. 1, p. 157, 2020.
[118] C. B. Meher-Homji and T. R. Mee, "Gas Turbine Power Augmentation By Fogging Of Inlet Air," in *Proceedings of the 28th Turbomachinery Symposium*, 1999: Texas A&M University. Turbomachinery Laboratories.
[119] J. R. Khan, "Fog cooling, wet compression and droplet dynamics in gas turbine compressors," 2009.
[120] J. Yao and H. Liu, "The experimental research of effects of roughness on the turbine cascade loss coefficient," *Gas Turbine Technology,* vol. 21, no. 2, pp. 28-31, 2006.
[121] J. Wen, G.-L. Zhao, L.-D. He, and H. Peng, "Effects of non-smooth blades on the cascade exit streamwise vortex systems," *Journal of Aerospace Power,* vol. 16, no. 3, pp. 283-286, 2001.
[122] T. Bai, J. Liu, W. Zhang, and Z. Zou, "Effect of surface roughness on the aerodynamic performance of turbine blade cascade," *Propulsion and Power Research,* vol. 3, no. 2, pp. 82-89, 2014.
[123] K. Bammert and H. Sandstede, "Measurements of the boundary layer development along a turbine blade with rough surfaces," 1980.
[124] J. Boynton, R. Tabibzadeh, and S. Hudson, "Investigation of rotor blade roughness effects on turbine performance," 1993.
[125] Y. I. Yun, I. Y. Park, and S. J. Song, "Performance degradation due to blade surface roughness in a single-stage axial turbine," *J. Turbomach.,* vol. 127, no. 1, pp. 137-143, 2005.
[126] R. Boyle, "Prediction of surface roughness and incidence effects on turbine performance," 1994.
[127] R. Boyle and R. Senyitko, "Measurements and predictions of surface roughness effects on the turbine vane aerodynamics," in *ASME Turbo Expo 2003, collocated with the 2003 International Joint Power Generation Conference*, 2003: American Society of Mechanical Engineers Digital Collection, pp. 291-303.
[128] J. D. Denton, "The 1993 IGTI scholar lecture: Loss mechanisms in turbomachines," 1993.
[129] M. Montis, R. Niehuis, and A. Fiala, "Effect of surface roughness on loss behaviour, aerodynamic loading and boundary layer development of a low-pressure gas turbine airfoil," in *ASME Turbo Expo 2010: Power for Land, Sea, and Air*, 2010: American Society of Mechanical Engineers Digital Collection, pp. 1535-1547.
[130] M. Montis, R. Niehuis, and A. Fiala, "Aerodynamic measurements on a low pressure turbine cascade with different levels of distributed roughness," in *ASME 2011 Turbo Expo: Turbine*

Technical Conference and Exposition, 2011: American Society of Mechanical Engineers Digital Collection, pp. 457-467.

[131] K. L. Suder, R. V. Chima, A. J. Strazisar, and W. B. Roberts, "The effect of adding roughness and thickness to a transonic axial compressor rotor," 1995.

[132] A. Suman, A. Fortini, N. Aldi, M. Merlin, and M. Pinelli, "A Shape Memory Alloy-Based Morphing Axial Fan Blade—Part II: Blade Shape and Computational Fluid Dynamics Analyses," *Journal of Engineering for Gas Turbines and Power,* vol. 138, no. 6, 2016.

[133] X. Weiwei, Z. Konghao, W. Jianjun, L. Yajun, and L. Qiang, "Modeling and numerical analysis of the effect of blade roughness on particle deposition in a flue gas turbine," *Powder Technology,* vol. 347, pp. 59-65, 2019.

[134] A. Suman, N. Casari, E. Fabbri, L. di Mare, F. Montomoli, and M. Pinelli, "Generalization of particle impact behavior in gas turbine via non-dimensional grouping," *Progress in Energy and Combustion Science,* vol. 74, pp. 103-151, 2019.

[135] J. Harris, B. Dempster, S. Sun, and M. Brandt, "Laser cladding repair of LP steam turbine blades," in *PICALO 2006 Conference Proceedings*, 2006.

[136] C. Kwok, H. Man, F. Cheng, and K. Lo, "Developments in laser-based surface engineering processes: with particular reference to protection against cavitation erosion," *Surface and Coatings Technology,* vol. 291, pp. 189-204, 2016.

[137] J. Lee and F. Zhao, "Global Wind Report 2019," Global Wind Energy Council;, 2020.

[138] R. A. Kishore, "Small-scale Wind Energy Portable Turbine (SWEPT)," Master of Science, Mechanical Engineering, Virginia Polytechnic Institute and State University, 2013.

[139] O. Cleynen. Wing profile nomenclature [Online] Available: https://en.wikipedia.org/wiki/Airfoil

[140] N. Boccard, "Capacity factor of wind power realized values vs. estimates," *energy policy,* vol. 37, no. 7, pp. 2679-2688, 2009.

[141] K. R. Ram, S. Lal, and M. Rafiuddin Ahmed, "Low Reynolds number airfoil optimization for wind turbine applications using genetic algorithm," *Journal of Renewable and Sustainable Energy,* vol. 5, no. 5, p. 052007, 2013.

[142] N. Karthikeyan, K. K. Murugavel, S. A. Kumar, and S. Rajakumar, "Review of aerodynamic developments on small horizontal axis wind turbine blade," *Renewable and Sustainable Energy Reviews,* vol. 42, pp. 801-822, 2015.

[143] E. White *et al.*, "Leading-Edge Roughness Effects on 63 (3)-418 Airfoil Performance," in *49th AIAA Aerospace Sciences Meeting including the New Horizons Forum and Aerospace Exposition*, 2011, p. 352.

[144] N. Dalili, A. Edrisy, and R. Carriveau, "A review of surface engineering issues critical to wind turbine performance," *Renewable and Sustainable energy reviews,* vol. 13, no. 2, pp. 428-438, 2009.

[145] C. M. Langel *et al.*, "Analysis of the impact of leading edge surface degradation on wind turbine performance," in *33rd Wind Energy Symposium*, 2015, p. 0489.

[146] R. S. Ehrmann and E. White, "Effect of Blade Roughness on Transition and Wind Turbine Performance," Sandia National Lab.(SNL-NM), Albuquerque, NM (United States), 2015.

[147] M. Schramm, H. Rahimi, B. Stoevesandt, and K. Tangager, "The influence of eroded blades on wind turbine performance using numerical simulations," *Energies,* vol. 10, no. 9, p. 1420, 2017.

[148] H. Im and B. Kim, "Numerical study on the effect of blade surface deterioration by erosion on the performance of a large wind turbine," *Journal of Renewable and Sustainable Energy,* vol. 11, no. 6, p. 063308, 2019.

[149] N. Gaudern, "A practical study of the aerodynamic impact of wind turbine blade leading edge erosion," in *Journal of Physics: Conference Series*, 2014, vol. 524, no. 1: IOP Publishing, p. 012031.

[150] R. Gutiérrez, E. Llórente, F. Echeverría, and D. Ragni, "Wind tunnel tests for vortex generators mitigating leading-edge roughness on a 30% thick airfoil," in *Journal of Physics: Conference Series*, 2020, vol. 1618, no. 5: IOP Publishing, p. 052058.

[151] O. Pires, X. Munduate, K. Boorsma, O. C. Yilmaz, H. A. Madsen, and W. Timmer, "Experimental investigation of surface roughness effects and transition on wind turbine performance," in *J. Phys.: Conf. Ser*, 2018, vol. 1037, p. 052018.

[152] A. Sareen, C. A. Sapre, and M. S. Selig, "Effects of leading edge erosion on wind turbine blade performance," *Wind Energy,* vol. 17, no. 10, pp. 1531-1542, 2014.

[153] W. J. Jasinski, S. C. Noe, M. S. Selig, and M. B. Bragg, "Wind turbine performance under icing conditions," 1998.

[154] S. Barber, Y. Wang, S. Jafari, N. Chokani, and R. S. Abhari, "The impact of ice formation on wind turbine performance and aerodynamics," *Journal of Solar Energy Engineering,* vol. 133, no. 1, 2011.

[155] L. Talhaug, K. Vindteknik, G. Ronsten, R. Horbaty, I. Baring-Gould, and A. Lacroix, "Wind energy projects in cold climates," *Executive Committee of the International Energy Agency Program for Research and Development on Wind Energy Conversion Systems,* pp. 1-36, 2005.

[156] L. Gao, R. Veerakumar, Y. Liu, and H. Hu, "Quantification of the 3D shapes of the ice structures accreted on a wind turbine airfoil model," *Journal of Visualization,* vol. 22, no. 4, pp. 661-667, 2019.

[157] G. P. Corten, "Flow separation on wind turbine blades," *University of Utrecht,* 2001.

[158] F. Trieb, "Interference of Flying Insects and Wind Parks. Study Report," *Deutsches Zentrum für Luft-und Raumfahrt (DLR),* 2018.

[159] B. F. Sørensen, E. Jørgensen, C. P. Debel, H. M. Jensen, T. K. Jacobsen, and K. Halling, "Improved design of large wind turbine blade of fibre composites based on studies of scale effects (Phase 1). Summary Report," 2004.

[160] L. Bartolomé and J. Teuwen, "Prospective challenges in the experimentation of the rain erosion on the leading edge of wind turbine blades," *Wind Energy,* vol. 22, no. 1, pp. 140-151, 2019.

[161] R. Herring, K. Dyer, F. Martin, and C. Ward, "The increasing importance of leading edge erosion and a review of existing protection solutions," *Renewable and Sustainable Energy Reviews,* vol. 115, p. 109382, 2019.

[162] L. Mishnaevsky Jr, "Repair of wind turbine blades: Review of methods and related computational mechanics problems," *Renewable energy,* 2019.

[163] S. Arunvinthan, S. N. Pillai, and S. Cao, "Aerodynamic characteristics of variously modified leading-edge protuberanced (LEP) wind turbine blades under various turbulent intensities," *Journal of Wind Engineering and Industrial Aerodynamics,* vol. 202, p. 104188, 2020.

[164] S. Campobasso, "Accounting for uncertainty in offshore wind economics: the case of blade leading edge erosion," in *Webinar of the institution of mechanical engineers*, 2020.

[165] K. Gunn and C. Stock-Williams, "Quantifying the global wave power resource," *Renewable Energy,* vol. 44, pp. 296-304, 2012.

[166] R. H. Charlier, "A “sleeper” awakes: tidal current power," *Renewable and Sustainable Energy Reviews,* vol. 7, no. 6, pp. 515-529, 2003.

[167] D. Li, S. Wang, and P. Yuan, "An overview of development of tidal current in China: energy resource, conversion technology and opportunities," *Renewable and Sustainable Energy Reviews,* vol. 14, no. 9, pp. 2896-2905, 2010.

[168] R. Pelc and R. M. Fujita, "Renewable energy from the ocean," *Marine Policy,* vol. 26, no. 6, pp. 471-479, 2002.

[169] M. H. Khanjanpour and A. A. Javadi, "Experimental and CFD Analysis of Impact of Surface Roughness on Hydrodynamic Performance of a Darrieus Hydro (DH) Turbine," *Energies,* vol. 13, no. 4, p. 928, 2020.

[170] S. Song, W. Shi, Y. K. Demirel, and M. Atlar, "The effect of biofouling on the tidal turbine performance," in *Applied Energy Symposium*, 2019.
[171] J. M. Walker, K. A. Flack, E. E. Lust, M. P. Schultz, and L. Luznik, "Experimental and numerical studies of blade roughness and fouling on marine current turbine performance," *Renewable Energy,* vol. 66, pp. 257-267, 2014.
[172] P. L. Fraenkel, "Power from marine currents," *Proceedings of the Institution of Mechanical Engineers, Part A: Journal of Power and Energy,* vol. 216, no. 1, pp. 1-14, 2002.
[173] K.-W. Ng, W.-H. Lam, and K.-C. Ng, "2002–2012: 10 years of research progress in horizontal-axis marine current turbines," *Energies,* vol. 6, no. 3, pp. 1497-1526, 2013.
[174] Pearson College UWC. "6-Month Fouling Records on Tidal Energy Turbine from the Race Rocks Ecological Reserve, https://www.racerocks.ca." (accessed 2021).
[175] J. Orme, I. Masters, and R. Griffiths, "Investigation of the effect of biofouling on the efficiency of marine current turbines," in *Proc. MAREC*, 2001, pp. 91-99.
[176] S. Song, Y. K. Demirel, M. Atlar, and W. Shi, "Prediction of the fouling penalty on the tidal turbine performance and development of its mitigation measures," *Applied Energy,* vol. 276, p. 115498, 2020/10/15/ 2020, doi: https://doi.org/10.1016/j.apenergy.2020.115498.
[177] J. S. Walker, R. B. Green, E. A. Gillies, and C. Phillips, "The effect of a barnacle-shaped excrescence on the hydrodynamic performance of a tidal turbine blade section," *Ocean Engineering,* vol. 217, p. 107849, 2020/12/01/ 2020, doi: https://doi.org/10.1016/j.oceaneng.2020.107849.
[178] J. Carlton, *Marine propellers and propulsion*. Butterworth-Heinemann, 2018.
[179] M. Schultz, J. Bendick, E. Holm, and W. Hertel, "Economic impact of biofouling on a naval surface ship," *Biofouling,* vol. 27, no. 1, pp. 87-98, 2011.
[180] P. Kellett, K. Mizzi, Y. Demirel, and O. Turan, "Investigating the roughness effect of biofouling on propeller performance," in *International Conference on Shipping in Changing Climates*, 2015.
[181] J. Lichtman, D. Kallas, C. Chatten, and C. E. COCHRAN JR, "Cavitation erosion of structural materials and coatings," *Corrosion,* vol. 17, no. 10, pp. 497t-505t, 1961.
[182] T. Okada, Y. Iwai, S. Hattori, and N. Tanimura, "Relation between impact load and the damage produced by cavitation bubble collapse," *Wear,* vol. 184, no. 2, pp. 231-239, 1995.
[183] M. Suner and O. Birdal, "Effect of Cavitation in Ships on the Environment," in *Causes, Impacts and Solutions to Global Warming*: Springer, 2013, pp. 957-973.
[184] C. E. Brennen, *Cavitation and bubble dynamics*. Cambridge University Press, 2014.
[185] W. Cong *et al.*, "An experimental investigation of the composite coating for marine propellers on cavitation characteristics and fouling release property," in *IOP Conference Series: Materials Science and Engineering*, 2019, vol. 504, no. 1: IOP Publishing, p. 012030.
[186] C. S. Subramanian, T. M. Ostrem, and S. N. Gangadharan, "Noncontact measurement of marine biofouling roughness," *Marine Technology,* vol. 41, no. 2, pp. 67-73, 2004.